

# Novel *N*-Benzoyl-2-Hydroxybenzamide Disrupts Unique Parasite Secretory Pathway

Alina Fomovska,<sup>a</sup> Qingqing Huang,<sup>\*b</sup> Kamal El Bissati,<sup>a</sup> Ernest J. Mui,<sup>a</sup> William H. Witola,<sup>\*a</sup> Gang Cheng,<sup>b</sup> Ying Zhou,<sup>a</sup> Caroline Sommerville,<sup>c</sup> Craig W. Roberts,<sup>c</sup> Sam Bettis,<sup>a</sup> Sean T. Prigge,<sup>d</sup> Gustavo A. Afanador,<sup>d</sup> Mark R. Hickman,<sup>e</sup> Patty J. Lee,<sup>e</sup> Susan E. Leed,<sup>e</sup> Jennifer M. Auschwitz,<sup>e</sup> Marco Pieroni,<sup>\*b</sup> Jozef Stec,<sup>b</sup> Stephen P. Muench,<sup>f</sup> David W. Rice,<sup>g</sup> Alan P. Kozikowski,<sup>b</sup> and Rima McLeod<sup>a</sup>

Department of Ophthalmology and Visual Sciences, Pediatrics (Infectious Diseases), Committees on Genetics, Immunology, and Molecular Medicine, Institute of Genomics and Systems Biology, and The College, The University of Chicago, Chicago, Illinois, USA<sup>a</sup>; Drug Discovery Program, Department of Medicinal Chemistry and Pharmacognosy, University of Illinois at Chicago, Chicago, Illinois, USA<sup>b</sup>; Strathclyde Institute of Pharmacy & Biomedical Sciences, University of Strathclyde, Glasgow, United Kingdom<sup>c</sup>; Johns Hopkins School of Public Health, Baltimore, Maryland, USA<sup>d</sup>; Department of Discovery, Division of Experimental Therapeutics, Walter Reed Army Institute of Research, Silver Spring, Maryland, USA<sup>e</sup>; Institute of Membrane and Systems Biology, University of Leeds, Leeds, United Kingdom<sup>f</sup>; and Department of Molecular Biology, University of Sheffield, Sheffield, United Kingdom<sup>g</sup>

***Toxoplasma gondii* is a protozoan parasite that can damage the human brain and eyes. There are no curative medicines. Herein, we describe our discovery of *N*-benzoyl-2-hydroxybenzamides as a class of compounds effective in the low nanomolar range against *T. gondii* *in vitro* and *in vivo*. Our lead compound, QQ-437, displays robust activity against the parasite and could be useful as a new scaffold for development of novel and improved inhibitors of *T. gondii*. Our genome-wide investigations reveal a specific mechanism of resistance to *N*-benzoyl-2-hydroxybenzamides mediated by adaptin-3 $\beta$ , a large protein from the secretory protein complex. *N*-Benzoyl-2-hydroxybenzamide-resistant clones have alterations of their secretory pathway, which traffics proteins to micronemes, rhoptries, dense granules, and acidocalcisomes/plant-like vacuole (PLVs). *N*-Benzoyl-2-hydroxybenzamide treatment also alters micronemes, rhoptries, the contents of dense granules, and, most markedly, acidocalcisomes/PLVs. Furthermore, QQ-437 is active against chloroquine-resistant *Plasmodium falciparum*. Our studies reveal a novel class of compounds that disrupts a unique secretory pathway of *T. gondii*, with the potential to be used as scaffolds in the search for improved compounds to treat the devastating diseases caused by apicomplexan parasites.**

*Toxoplasma gondii* is an apicomplexan, intracellular parasite that infects one third to one half of the world's population. It can cause eye and brain disease and death, and the presence of infection has been correlated with a variety of neurologic illnesses. Moreover, it is the most frequent cause of infectious uveitis worldwide. Disease can be especially severe in immunocompromised persons and in those infected congenitally (28).

There is no perfect treatment for *T. gondii* infection in humans, as the few available medicines are limited by their side effects and target only the rapidly proliferating tachyzoite form of the parasite. Pyrimethamine and sulfadiazine, which are effective against the tachyzoite form, are currently used to treat active disease. However, treatment with these medicines can be associated with toxicity and hypersensitivity (29), and they do not eradicate the bradyzoite form of the parasite, which remains latent. There are few secondary medicines, and some of them have a delayed mechanism of killing the tachyzoites. No medicines have been reported to be effective against the latent, encysted bradyzoite stage. *T. gondii* remains in a person's body throughout life, leading to a risk for recurrence of active infection. Novel, effective, and nontoxic anti-*Toxoplasma* agents are urgently needed. Herein, we present a series of experiments to identify new lead compounds effective against *T. gondii* and to begin to understand how they act on this parasite.

## MATERIALS AND METHODS

**Parasites and cell culture.** Confluent monolayers of human foreskin fibroblasts (HFF) were maintained in Iscove's modified Dulbecco's medium supplemented with 10% fetal bovine serum, 1% Glutamax, and 1%

penicillin-streptomycin-amphotericin B (Fungizone) (IMDM-C) at 33°C or 37°C and 5% CO<sub>2</sub>. *Toxoplasma gondii* parasites were maintained in HFF monolayers under the conditions described above. The strains of parasite used in this study include RH, RH-YFP (kindly provided by Boris Streipen, University of Georgia), and Prugneaud Fluc (type 2 parasites stably transfected with luciferase, kindly provided by Seon Kim, Jeroen Saeij, and John Boothroyd [Stanford University] and Laura Knoll [University of Wisconsin, Madison, Wisconsin]).

**High-throughput screen.** A high-throughput screen of a library optimized for its absorption, distribution, metabolism, excretion, and toxicity (ADMET) properties was carried out as described below for *in vitro* challenge and toxicity assays.

**Synthesis of derivatives of MP-IV-1 and QQ-437.** MP-IV-1 and QQ-437 were synthesized to develop novel inhibitors of *T. gondii* for this work.

Received 24 December 2011 Returned for modification 7 February 2012

Accepted 13 February 2012

Published ahead of print 21 February 2012

Address correspondence to Rima McLeod, rmcLeod@uchicago.edu.

\* Present address: Q. Huang, Institute of Drug Discovery and Development, iAIR, Shanghai Engineering Research Center of Molecular Therapeutics and New Drug Development, East China Normal University, Shanghai, People's Republic of China; W. H. Witola, Department of Agricultural and Environmental Sciences, Tuskegee University, Tuskegee, Alabama, USA; M. Pieroni, Centro Interdipartimentale Biopharmaceutico, Campus Universitario, Università di Parma, Parma, Italy. A.F. and Q.H. contributed equally to this article.

Supplemental material for this article may be found at <http://aac.asm.org/>.

Copyright © 2012, American Society for Microbiology. All Rights Reserved.

doi:10.1128/AAC.06450-11

They were repurposed to test against the K1 isolate of *P. falciparum* with *Leishmania* and trypanosomes to compare the structure-activity relationship (SAR) for each of those. The details of a number of these syntheses are described elsewhere (42a). The compounds synthesized are shown in Table 1. Additional details of syntheses and analysis not included in reference 42a are as follows.

(i) ***N*-Benzoyl-4-ethylbenzamide (chg-1-13)**. To a solution of benzamide (121 mg, 1 mmol) in 2 ml pyridine, 4-ethylbenzoyl chloride (1 mmol) was added dropwise at 0°C. The mixture was stirred for 10 h at room temperature, diluted with ethyl acetate, washed with water, and concentrated. The residue was purified by flash chromatography (silica gel, 25% ethyl acetate [EtOAc]-hexane) to give compound chg-1-13 (177 mg, 70%). <sup>1</sup>H nuclear magnetic resonance (NMR) (CDCl<sub>3</sub>) δ 8.85 (s, 1H), 7.88 (d, *J* = 7.2 Hz, 2H), 7.81 (d, *J* = 8.0 Hz, 2H), 7.65 (t, *J* = 7.2 Hz, 1H), 7.53 (t, *J* = 7.2 Hz, 2H), 7.35 (d, *J* = 8.0 Hz, 2H), 2.75 (q, *J* = 7.2 Hz, 2H), 1.29 (t, *J* = 7.2 Hz, 3H); <sup>13</sup>C NMR (CDCl<sub>3</sub>) δ 166.5, 166.2, 149.6, 133.1, 132.5, 130.3, 128.3, 127.9, 127.8, 127.7, 28.5, 14.8; high-pressure liquid chromatography (HPLC) purity, 97.7%.

(ii) ***N*-Benzoyl-4-diethylaminobenzamide (chg-1-17b)**. Following the same procedure as that for chg-1-13, to a solution of benzamide (121 mg, 1 mmol) in 2 ml pyridine, 4-diethylaminobenzoyl chloride (1 mmol) in pyridine (1 ml) was added dropwise at 0°C. The mixture was stirred for 10 h at room temperature, diluted with ethyl acetate, washed with water, and concentrated. The residue was purified by flash chromatography (silica gel, 30% EtOAc-hexane) to give compound chg-1-17b (44 mg, 15%). <sup>1</sup>H NMR (CDCl<sub>3</sub>) δ 8.73 (s, 1H), 7.85 (d, *J* = 7.6 Hz, 2H), 7.80 (d, *J* = 8.8 Hz, 2H), 7.59 (t, *J* = 7.2 Hz, 1H), 7.49 (t, *J* = 7.2 Hz, 2H), 6.67 (d, *J* = 8.8 Hz, 2H), 3.44 (q, *J* = 6.8 Hz, 4H), 1.23 (t, *J* = 7.2 Hz, 6H); <sup>13</sup>C NMR (CDCl<sub>3</sub>) δ 166.7, 165.0, 150.9, 133.8, 132.2, 130.1, 128.3, 127.5, 118.0, 110.1, 44.2, 12.1; HPLC purity, 98.5%.

(iii) ***N*-(4-Ethylbenzoyl)-2-methoxybenzenesulfonamide (chg-1-19)**. To a solution of 5-bromo-2-methoxybenzenesulfonyl chloride (250 mg, 0.88 mmol) in tetrahydrofuran (THF) (3 ml) was added 1 ml NH<sub>4</sub>OH aqueous solution (28% to 35%). The mixture was stirred at room temperature for 10 h. The solvent was removed under reduced pressure, diluted with ethyl acetate, washed with water twice, dried, and concentrated to yield 5-bromo-2-methoxybenzenesulfonamide (212 mg, 91%). <sup>1</sup>H NMR (dimethyl sulfoxide [DMSO]-*d*<sub>6</sub>) δ 7.79 to 7.73 (m, 2H), 7.25 (s, 2H) 7.19 (d, *J* = 8.8 Hz, 1H), 3.90 (s, 3H).

A mixture of 5-bromo-2-methoxybenzenesulfonamide (212 mg, 0.8 mmol), Pd/C (10%, 20 mg) in 5 ml methanol (MeOH) was vigorously stirred for 10 h under H<sub>2</sub> (1 atm) at room temperature. The mixture was filtered through a pad of Celite to remove Pd/C. The filtrate was concentrated to give 2-methoxybenzenesulfonamide (150 mg, 100%). <sup>1</sup>H NMR (DMSO-*d*<sub>6</sub>) δ 7.74 (d, *J* = 8.0 Hz, 1H), 7.56 (d, *J* = 8.0 Hz, 1H), 7.20 (d, *J* = 8.0 Hz, 1H), 7.10 to 7.00 (m, 3H), 3.93 (s, 3H).

To a mixture of 2-methoxybenzenesulfonamide (150 mg, 0.8 mmol), K<sub>2</sub>CO<sub>3</sub> (207 mg, 1.5 mmol) in THF (4 ml) was added 4-ethylbenzoic chloride (0.15 ml, 1 mmol), and then the solution was heated to 60°C for 5 h. A white solid was precipitated after addition of ethyl acetate (5 ml) and water (5 ml). The white solid was collected by filtration to give the compound chg-1-19 (127 mg, 50%). <sup>1</sup>H NMR (CDCl<sub>3</sub>) δ 9.11 (s, 1H), 8.21 (m, 1H), 7.75 (m, 2H), 7.60 (m, 1H), 7.28 (m, 1H), 7.18 (m, 1H), 7.02 (m, 1H), 3.95 (s, 3H), 2.65 (m, 2H), 1.25 (m, 3H); <sup>13</sup>C NMR (CDCl<sub>3</sub>) δ 164.2, 156.5, 150.0, 135.5, 131.8, 128.4, 127.9, 127.8, 125.8, 120.2, 111.8, 55.8, 28.5, 14.7; HPLC purity, 98.1%.

(iv) ***N*-(4-Ethylbenzoyl)-2-hydroxybenzenesulfonamide (chg-1-22)**. To a solution of compound chg-1-19 (100 mg, 0.31 mmol) in dry dichloromethane, boron tribromide (1.1 mmol, 1 M in dichloromethane) was added dropwise at -78°C. The reaction mixture was stirred overnight at room temperature, quenched with 1 N HCl solution (3 ml) at 0°C, diluted with ethyl acetate, washed with water twice, dried over Na<sub>2</sub>SO<sub>4</sub>, and concentrated to give compound chg-1-22 (47 mg, 50%) as a white solid. <sup>1</sup>H NMR (DMSO-*d*<sub>6</sub>) δ 12.2 (brs, 1H), 10.8 (brs, 1H), 7.85 (m, 3H), 7.50 (m, 1H), 7.35 (m, 2H), 6.90 (m, 2H), 2.65 (m, 2H), 1.23 (m, 3H); <sup>13</sup>C

NMR (CDCl<sub>3</sub>) δ 165.2, 156.5, 150.7, 136.2, 128.9, 128.2, 127.6, 121.1, 119.9, 119.1, 99.6, 28.5, 14.7; HPLC purity, 96.5%.

(v) ***N*-(4-Diethylaminobenzoyl)-2-methoxybenzenesulfonamide (chg-1-23)**. To a solution of 2-methoxybenzamide (121 mg, 1 mmol) and 4-dimethylaminopyridine (DMAP) (293 mg, 2.4 mmol) in 2 ml pyridine, 4-ethylbenzoyl chloride (1 mmol) was added dropwise at 0°C. The mixture was stirred for 10 h at room temperature. White solid was precipitated after addition of ethyl acetate (5 ml) and water (5 ml). The solid was collected by filtration to give compound chg-1-23 (127 mg, 40%). <sup>1</sup>H NMR (DMSO-*d*<sub>6</sub>) δ 11.8 (brs, 1H), 7.90 (d, *J* = 8.0 Hz, 1H), 7.75 (d, *J* = 8.8 Hz, 2H), 7.65 (t, *J* = 8.0 Hz, 1H), 7.22 (d, *J* = 8.0 Hz, 1H), 7.13 (t, *J* = 8.0 Hz, 1H), 6.63 (d, *J* = 8.8 Hz, 2H), 3.83 (s, 3H), 3.40 (q, *J* = 6.8 Hz, 4H), 1.09 (d, *J* = 6.8 Hz, 6H); <sup>13</sup>C NMR (DMSO-*d*<sub>6</sub>) δ 164.0, 156.8, 151.3, 135.4, 132.0, 130.1, 126.7, 120.6, 116.7, 112.1, 110.4, 56.2, 44.5, 12.4; HPLC purity, 99.1%.

(vi) ***N*-(4-Diethylaminobenzoyl)-2-hydroxybenzenesulfonamide (chg-1-24)**. To a solution of compound chg-1-23 (100 mg, 0.31 mmol) in dry dichloromethane was added dropwise a boron tribromide solution in dichloromethane (1.1 ml, 1 M in dichloromethane) at -78°C. The reaction mixture was stirred overnight at room temperature, quenched with 1 N NaHCO<sub>3</sub> solution (3 ml) at 0°C, diluted with ethyl acetate, washed with water twice, dried over Na<sub>2</sub>SO<sub>4</sub>, and concentrated. The residue was purified through preparative HPLC to give compound chg-1-24 (32 mg, 30%) as white solid. <sup>1</sup>H NMR (CD<sub>3</sub>OD) δ 7.89 (d, *J* = 8.0 Hz, 1H), 7.72 (d, *J* = 9.2 Hz, 2H), 7.48 (t, *J* = 8.0 Hz, 1H), 7.00 (m, 2H), 6.69 (d, *J* = 8.8 Hz, 2H), 3.45 (q, *J* = 6.8 Hz, 4H), 1.18 (d, *J* = 6.8 Hz, 6H); <sup>13</sup>C NMR (CD<sub>3</sub>OD) δ 166.6, 155.8, 151.5, 135.0, 130.1, 124.6, 118.9, 117.2, 116.6, 110.1, 44.0, 11.3; HPLC purity, >99%.

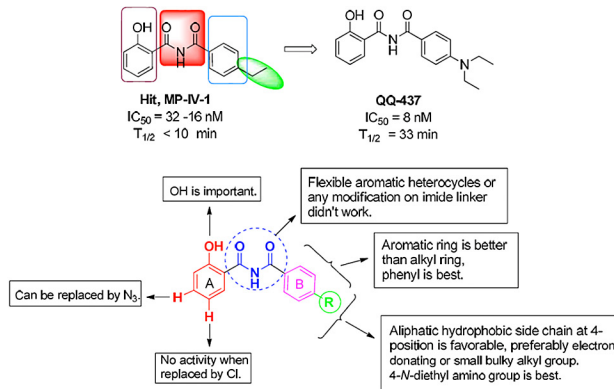
(vii) ***N*-(4-Ethylbenzoyl)-2-methoxybenzamide (chg-1-27)**. To a solution of 2-methoxybenzamide (121 mg, 1 mmol) in 2 ml pyridine, 4-ethylbenzoyl chloride (1 mmol) was added dropwise at 0°C. The mixture was stirred for 10 h at room temperature, diluted with ethyl acetate, washed with water and concentrated. The residue was purified by flash chromatography (silica gel, 30% EtOAc/Hexane) to give compound chg-1-27 (85 mg, 30%). <sup>1</sup>H NMR (CDCl<sub>3</sub>) δ 11.21 (s, 1H), 8.28 (d, *J* = 8.0 Hz, 1H), 7.84 (d, *J* = 8.0 Hz, 2H), 7.55 (t, *J* = 8.0 Hz, 1H), 7.33 (d, *J* = 8.0 Hz, 2H), 7.10 (t, *J* = 8.0 Hz, 1H), 7.05 (d, *J* = 8.0 Hz, 1H), 4.10 (s, 3H), 2.74 (q, *J* = 7.2 Hz, 2H), 1.28 (t, *J* = 7.2 Hz, 3H); <sup>13</sup>C NMR (CDCl<sub>3</sub>) δ 164.8, 162.6, 157.0, 149.4, 134.2, 132.9, 131.1, 128.0, 127.3, 121.6, 120.5, 111.3, 56.2, 28.5, 14.8; HPLC purity, >99%.

(viii) **4-Ethyl-*N*-(2-hydroxybenzoyl)benzenesulfonamide (chg-1-28)**. To a mixture of 4-ethylbenzenesulfonamide (300 mg, 1.66 mmol), K<sub>2</sub>CO<sub>3</sub> (455 mg, 3.3 mmol) in THF (4 ml) 2-benzyloxybenzoyl chloride (409, 1.66 mmol) was added, and the solution was heated to 60°C for 5 h, diluted with ethyl acetate (30 ml), washed with water twice, and concentrated. The crude intermediate was redissolved with 10 ml MeOH and hydrogenated with Pd/C (10%, 10 mg) under H<sub>2</sub> (1 atm) for 5 h. Pd/C was removed by filtration. The filtrate was concentrated and purified by preparative HPLC to afford compound chg-1-28 (152 mg, 30%) as a white solid. <sup>1</sup>H NMR (CDCl<sub>3</sub>) δ 10.85 (brs, 1H), 9.80 (brs, 1H), 8.09 (d, *J* = 8.4 Hz, 2H), 7.65 (d, *J* = 8.0 Hz, 1H), 7.45 (m, 3H), 6.95 (d, *J* = 8.0 Hz, 1H), 6.85 (d, *J* = 8.0 Hz, 1H), 2.75 (q, *J* = 7.6 Hz, 2H), 1.27 (t, *J* = 7.6 Hz, 3H); <sup>13</sup>C NMR (CDCl<sub>3</sub>) δ 167.7, 161.4, 151.3, 135.9, 134.9, 128.4, 128.2, 127.1, 119.3, 118.3, 112.3, 28.8, 14.6; HPLC purity, >99%.

(ix) ***N*-(2-Hydroxybenzoyl)-4-isopropoxybenzamide (chg-1-43)**. Similar to the synthesis of QQ-437, a mixture of salicylamide (3 mmol) and 4-isopropoxybenzoyl chloride (3 mmol) in 6 ml pyridine was refluxed for 1 h. Chg-1-43 (628 mg, 70%) was obtained by recrystallization from methanol, ethyl acetate, and water. <sup>1</sup>H NMR (DMSO-*d*<sub>6</sub>) δ 11.73 (s, 1H), 11.58 (s, 1H), 7.87 (m, 3H), 7.46 (t, *J* = 8.0 Hz, 1H), 7.03 (m, 4H), 4.76 (m, 1H), 1.09 (d, *J* = 4.0 Hz, 6H); <sup>13</sup>C NMR (DMSO-*d*<sub>6</sub>) δ 164.2, 164.2, 161.4, 156.4, 134.2, 131.1, 130.0, 125.4, 120.0, 119.2, 117.1, 115.4, 69.8, 21.7; HPLC purity, >99%.

(x) ***N*-(2-Hydroxybenzoyl)-4-pyrrolidin-1-ylbenzamide (chg-1-46)**. Similar to the synthesis of QQ-437, a mixture of salicylamide (3 mmol)

TABLE 1 SAR based on inhibitory effects of *N*-benzoyl-2-hydroxybenzimidates on *T. gondii*<sup>a</sup>



Name	structure	MIC <sub>50</sub> (μM)	MIC <sub>90</sub> (μM)	TOX (μM)	Name	structure	MIC <sub>50</sub> (μM)	MIC <sub>90</sub> (μM)	TOX (μM)	Name	structure	MIC <sub>50</sub> (μM)	MIC <sub>90</sub> (μM)	TOX (μM)
MP-IV-1		0.031-0.016	0.062-0.031	>10	MP-IV-32		>1	>10	>10	JS-1-51		>1	N.D.	N.D.
QQ-437		0.016-0.008	0.016-0.008	>0.25	MP-IV-14		1-0.1	>1	>1	JS-1-52		>1	N.D.	N.D.
MP-IV-28		0.01-0.001	0.1-0.01	>1	MP-IV-15		>1	>1	>1	JS-1-73		>1	N.D.	N.D.
QQ-411		0.1-0.01	0.1-0.01	N.D.	JS-1-99		>1	N.D.	N.D.	JS-1-79		>1	N.D.	N.D.
MP-IV-29		10 - 1	10 - 1	>10	JS-2-34		>1	N.D.	N.D.	JS-1-72		>1	N.D.	N.D.
JS-2-40		0.5-0.125	N.D.	N.D.	Chg-1-13		> 0.25	>0.250	>0.250	JS-1-58		>1	N.D.	N.D.
JS-2-38		1 - 0.5	N.D.	N.D.	chg-1-17b		0.25-0.125	>0.250	>0.25	JS-2-61		>0.25	N.D.	>0.25
MP-IV-16		1-0.1	>1	>1	QQ-440		> 0.25	N.D.	>0.25	JS-2-63		>0.25	N.D.	>0.25
JS-2-64		0.125-0.062	>0.25	>0.25	QQ-445		0.25-0.125	>0.25	>0.25	JS-2-65		>0.25	N.D.	>0.25
MP-IV-20		1-0.1	10 - 1	>1	QQ-423		0.125-0.062	>0.25	>0.25	JS-2-66		>0.25	N.D.	>0.25
QQ-416		1-0.1	N.D.	N.D.	JS-2-74		> 0.25	N.D.	>0.25	MP-IV-33		>1	>10	>10
QQ-421		0.062-0.031	0.125-0.062	>0.25	JS-2-84		> 0.25	N.D.	>0.25	JS-2-90		>0.25	N.D.	>0.25
QQ-439		0.062-0.031	0.125-0.25	>0.25	JS-2-93		> 0.125	N.D.	N.D.	JS-2-88		>0.25	N.D.	>0.25
chg-1-46		0.25-0.125	>0.25	>0.25	JS-3-07		> 0.125	>0.125	>0.125	MP-IV-13		>1	>1	>1
MP-IV-36		0.01-0.001	0.1-0.01	>1	QQ-448		> 0.125	>0.125	N.D.	JS-2-75		> 0.25	N.D.	>0.25
chg-1-43		0.062-0.125	>0.25	>0.25	QQ-450		> 0.125	>0.125	N.D.	JS-2-77		> 0.25	N.D.	>0.25
MP-IV-11		0.1-0.01	1 - 0.1	>1	QQ-428		> 0.25	N.D.	>0.25	chg-1-19		> 0.25	>0.260	>0.25
QQ-48		0.1-0.01	N.D.	N.D.	QQ-435		> 0.25	N.D.	>0.25	chg-1-27		>0.25	> 0.25	>0.25
QQ-49		0.1-0.01	0.1-0.01	N.D.	chg-1-22		> 0.25	>0.250	>0.250	chg-1-23		> 0.25	>0.260	>0.25
JS-2-64		0.125-0.062	>0.25	>0.25	chg-1-28		> 0.25	>0.250	>0.250	JS-2-56		>0.25	N.D.	>0.25
QQ-424		0.125-0.062	0.25-0.125	>0.25	QQ-412		>1	N.D.	N.D.	JS-2-79		>0.25	N.D.	>0.25
QQ-413		>1	N.D.	N.D.	MP-IV-24		10 - 1	10 - 1	>1	JS-2-81		>0.25	N.D.	>0.25
JS-2-67		>0.25	N.D.	>0.25	chg-1-24		>1	N.D.	N.D.					

<sup>a</sup> The diagram above the table body presents a summary of the SAR of *N*-benzoyl-2-hydroxybenzimidate inhibitors. The table shows the inhibitory effects of *N*-benzoyl-2-hydroxybenzimidates on *T. gondii* and the effects on host cells (toxicity). Analysis was also performed for *P. falciparum* KI and kinetoplastids (42a) for the compounds shown in the table. The range, where provided, reflects the small variability in the assay when replicate experiments were performed on different days. Also, some compounds were tested in parallel with QQ-437 but were not tested further upon being identified as inferior.

and 4-pyrrolidin-1-yl benzoyl chloride (3 mmol) in 6 ml pyridine was refluxed for 1 h. Chg-1-46 (558 mg, 60%) was obtained by recrystallization from methanol and water.  $^1\text{H}$  NMR (DMSO- $d_6$ )  $\delta$  11.77 (s, 1H), 11.47 (s, 1H), 7.90 (d,  $J$  = 8.0 Hz, 1H), 7.77 (d,  $J$  = 8.0 Hz, 2H), 7.46 (t,  $J$  = 8.0 Hz, 1H), 7.02 (m, 2H), 6.61 (d,  $J$  = 8.0 Hz, 2H), 3.33 (m, 4H), 1.99 (m, 4H);  $^{13}\text{C}$  NMR (DMSO- $d_6$ )  $\delta$  164.7, 164.4, 156.7, 151.0, 134.5, 131.5, 130.0, 120.4, 119.6, 119.4, 117.5, 111.5, 47.7, 25.4; HPLC purity, 97.3%.

**In vitro challenge and toxicity assays. (i) Initial screen of 6,811 compounds.** HFF were cultured in 19 384-well plates as described above. Cells were inoculated with RH-strain parasites, which express yellow fluorescent protein (RH-YFP), at a concentration of 3,500 parasites/ml. After incubation for 1 h, compounds were added to make the final concentration 10  $\mu\text{M}$  in singleton exemplars using the Tecan Freedom EVO 200 robotic platform. After 72 h, parasite proliferation was assessed using an ImageXpress Micro automated fluorescence microscope by measuring parasite fluorescence at a wavelength of 488 nm. Compounds were deemed effective if in their presence fluorescence was reduced to below 1,000 relative fluorescence units (RFU) at the end of the assay.

**(ii) Preparation of compounds for challenge and toxicity assays.** The initial 6,811-compound library was designed by Chris Lipinski and purchased by Alan Kozikowski at the University of Illinois at Chicago. Dilutions of 10 mM or 1 mM were made in DMSO, and further serial dilutions were made in IMDM-C. When cells or parasites were treated *in vitro*, the DMSO concentration was limited to 0.1%.

**(iii) Tachyzoite in vitro challenge assay.** RH parasites were separated from HFF by passage through a 25-gauge needle twice (32). Parasites were centrifuged at 1,500 rpm for 15 min, resuspended in IMDM-C, and counted. Confluent HFF in 96-well plates were inoculated with 3,500 parasites in a volume of 100  $\mu\text{l}$  per well. Parasites were allowed to infect cells for 1 h before inhibitory compounds and control medium were added. After 72 h, parasite burden was assessed with a YFP fluorescence assay or [ $^3\text{H}$ ]uracil incorporation assay.

In a YFP fluorescence assay, the relative fluorescence of parasite samples, which is directly correlated with parasite viability, was measured using a Synergy H4 hybrid reader (BioTek) and Gen5 1.10 software.

In a [ $^3\text{H}$ ]uracil incorporation assay (32), 25  $\mu\text{l}$  of 0.1-mCi/ml [ $^3\text{H}$ ]uracil was added to each well 48 h after initiation of the experiment. Twenty-four hours later, the contents of the wells were transferred onto 96-well filter plates using a cell harvester, and [ $^3\text{H}$ ]uracil incorporation, which is representative of parasite replication and viability, was measured using a liquid scintillation counter.

**(iv) Tachyzoite in vitro toxicity assay.** Toxicity to HFF was measured by means of a [ $^3\text{H}$ ]thymidine incorporation assay or a WST-1 cell viability assay.

In a [ $^3\text{H}$ ]thymidine incorporation assay, cells were cultured to  $\sim$ 30% confluence in 96-well plates. Inhibitory compounds and control medium were added at concentrations equal to those in challenge assays. Forty-eight hours later, 25  $\mu\text{l}$  of 0.1-mCi/ml [ $^3\text{H}$ ]thymidine was added to each well. Twenty-four hours after [ $^3\text{H}$ ]thymidine addition, cells were transferred onto 96-well filter plates using a cell harvester, and [ $^3\text{H}$ ]thymidine incorporation was measured using a liquid scintillation counter.

Toxicity assays also were conducted using WST-1 cell proliferation reagent (Roche). Confluent HFF were treated with inhibitory and control compounds at concentrations equal to those being tested in challenge assays. To assess cytotoxicity, on the day the samples were read, 10  $\mu\text{l}$  of WST-1 was added to each well, cells were incubated for 1 h, and absorbance was read using a fluorometer at 420 nm.

**Tachyzoite in vivo assays.** Compound efficacy *in vivo* in mice was determined according to two methods. In both cases compounds were first reconstituted in DMSO.

In the first method, SW mice were infected with 2,000 RH parasites by intraperitoneal injection. Mice were then treated with control solutions and with test compounds at various concentrations. Mice were sacrificed 5 or 6 days after infection, and the amount of parasites in the intraperito-

neal fluid was assessed. Four runs were conducted in total, each consisting of five groups of mice with four or five mice in each group.

In the second method, mice were infected intraperitoneally with 20,000 Fluc parasites in 400  $\mu\text{l}$  of phosphate-buffered saline (PBS) on day one. One hour later, mice were injected with either test compound at 20 mg/kg dissolved in 100  $\mu\text{l}$  of DMSO or a DMSO control. The test compound was administered daily for 6 days. Parasite burden was assessed by daily imaging with a Xenogen camera. This experiment was initiated with 4 or 5 mice per group; however, one mouse in the DMSO-only group and one in the QQ-437 group were omitted due to pregnancy, and one mouse in the QQ-437 20 mg/kg group died.

**Activity against Plasmodium falciparum.** Compound activity against *P. falciparum* was assessed using a malaria SYBR green I-based fluorescence (MSF) assay. Two laboratory strains of *P. falciparum* were used: D6 (Centers for Disease Control and Prevention [CDC]/Sierra Leone) and TM90-C235 (Walter Reed Army Institute of Research [WRAIR], Thailand). Parasites were maintained continuously in long-term cultures as previously described (22). Predosed microtiter drug plates for use in the MSF assay were produced using sterile 384-well black optical-bottom tissue culture plates containing dilutions of each test compound or chloroquine hydrochloride (Sigma-Aldrich Co.) suspended in DMSO. There were quadruplicate replicate wells for each of the 12 concentrations. There were serial twofold dilutions starting at 10,000 ng/ml for this dose-response test. The final concentration range tested was 0.5 to 10,000 ng/ml for all assays. Predosed plates were stored at 4°C until used, not to exceed 5 days. No difference was seen in drug sensitivity determinations between stored and fresh drug assay plates (data not shown). A batch control plate using chloroquine (Sigma-Aldrich Co.) at a final concentration of 2,000 ng/ml was used to validate each assay run. The Tecan Freedom EVO liquid handling system (Tecan US, Inc., Durham, NC) was used to produce all drug assay plates. Based on modifications of previously described methods (22, 36), *P. falciparum* strains in the late ring or early trophozoite stage were cultured in the predosed 384-well microtiter drug assay plates in a 38- $\mu\text{l}$  culture volume per well at a starting parasitemia of 0.3% and a hematocrit of 2%. The cultures were then incubated at 37°C with 5%  $\text{CO}_2$ , 5%  $\text{O}_2$ , and 90%  $\text{N}_2$  for 72 h. Lysis buffer (38  $\mu\text{l}$  per well), consisting of 20 mM Tris HCl, 5 mM EDTA, 1.6% Triton X, 0.016% saponin, and SYBR green I dye at a 20 $\times$  concentration (Invitrogen), was then added to the assay plates for a final SYBR green concentration of 10 $\times$ . The Tecan Freedom Evo liquid handling system was used to dispense malaria cell culture and lysis buffer. The plates were then incubated in the dark at room temperature for 24 h and examined for relative fluorescence units (RFU) per well using Tecan Genios Plus (Tecan US, Inc., Durham, NC). Each drug concentration was transformed into log[concentration] and plotted against the RFU values. The 50% and 90% inhibitory concentrations ( $\text{IC}_{50}$ s and  $\text{IC}_{90}$ s, respectively) were then generated with GraphPad Prism (GraphPad Software Inc., San Diego, CA) using the nonlinear regression (sigmoidal dose-response/variable slope) equation.

**Insertional mutagenesis. (i) Transfection of pLK47 plasmid into T. gondii.** The pLK47 vector plasmid (kindly provided by L. Knoll, Madison, WI) (23) was transfected into *T. gondii* parasites. Cytomix electroporation buffer solution, composed of 120 mM KCl, 150  $\mu\text{M}$   $\text{CaCl}_2$ , 5 mM  $\text{K}_2\text{HPO}_4$ , 5 mM  $\text{KH}_2\text{PO}_4$ , 25 mM HEPES, 2 mM EDTA, and 5 mM  $\text{MgCl}_2$  in water, was utilized. Strain RHdHxgPRT parasites were extracted from HFF by two subsequent passages through a 25-gauge needle, filtered, centrifuged for 5 min at 25,000 rpm, resuspended in 1 ml of Cytomix solution, and counted. A volume of Cytomix solution containing  $10 \times 10^7$  parasites and an equivalent amount of plasmid DNA were mixed to make up a total volume of 400  $\mu\text{l}$ . Immediately after mixing, parasites were pulsed using Bio-Rad electroporator at the following settings: 1.5 kV, 25  $\mu\text{F}$ , 100  $\Omega$ .

Parasites were grown in IMDM-C medium 37°C and 5%  $\text{CO}_2$  and treated with 25  $\mu\text{g}/\text{ml}$  mycophenolic acid and 50  $\mu\text{g}/\text{ml}$  xanthine. Medium was changed every other day. Parasites were grown in the presence of mycophenolic acid and xanthine for the duration of 1 month to ensure

the death of all parasites without the transfected plasmid. After 1 month, parasites were treated with MP-IV-1 at concentrations of 10  $\mu$ M, 0.5  $\mu$ M, and 0.03  $\mu$ M. Parasites were treated with MP-IV-1 for 2 weeks to ensure the death of all parasites not resistant to MP-IV-1.

**(ii) Cloning parasites to isolate individual mutants.** A bulk culture of parasites resistant to MP-IV-1 was diluted to a concentration of 1 parasite/100  $\mu$ l. A 96-well plate was inoculated with that concentration to yield 1 parasite/well. Parasites were treated with 10  $\mu$ M MP-IV-1 and incubated for 2 weeks. Wells with a single infection locus were selected and numbered A1 to A23. The contents were transferred to individual wells of 12-well plates. These parasites were cultured at 37°C and 5% CO<sub>2</sub> in the presence of 10  $\mu$ M MP-IV-1.

**(iii) Identification of genes that, when disrupted, confer resistance to MP-IV-1.** MP-IV-1-resistant parasite mutants were propagated in a T75 flask. DNA was extracted using DNAzol reagent and resuspended in water. Initial digestion was carried out with the restriction enzymes SalI, SacII, and NotI (each separately). Three microliters of restriction enzyme and 2  $\mu$ l of appropriate buffer were added to 20  $\mu$ l of each DNA sample. DNA was incubated overnight in a 37°C water bath. After purification of the DNA via phenol extraction, fragments were religated by adding 4  $\mu$ l T2 DNA ligase enzyme buffer at a 5 $\times$  strength and 1.5  $\mu$ l T4 ligase enzyme and refrigerating overnight at 4°C. After another phenol extraction, fragments were digested with a second set of enzymes paired with the first set as follows: SalI-NheI, SacI-MluI, NotI-NcoI. Inverse PCR was performed using forward and reverse primers corresponding to the second set of restriction enzymes. Primers are as follows: NheI inverse forward, 5'-AAGCGACGTTGTGTCTCAAATCRCRGAT-3'; NheI inverse reverse, 5'-ATGATGGCCGGACAAACAACAGATAA-3'; MluI inverse forward, 5'-ATTACCGCCTTGTAGTGAGCTGATA-3'; MluI inverse reverse, 5'-ACACAGCACCCGAACCTACGGAGCTGGT-3'; NcoI inverse forward, 5'-ATCGTGGTCTACGAGGCCACACTCA-3'; and NcoI inverse reverse, 5'-TCGCTGTAGCCGTCGCTCATAGCAAT-3'.

Amplification of fragments was confirmed by means of gel electrophoresis. Bright bands were cut out, and DNA was extracted from the gel with a Wizard SV gel and PCR cleanup system kit (Promega). DNA fragments were subsequently ligated into vector pGEMT and transfected into *Escherichia coli*. Bacterial colonies were screened to ensure integration of the plasmid vector by means of gel electrophoresis. Appropriate colonies were sent for sequencing.

The sequences obtained were analyzed using MacVector and BLAST at ToxoDB.org.

**Electron microscopy experiments.** HFF were cultured on carbon-coated glass coverslips obtained from Juan Jimenez (Albert Einstein University) in 24-well plates. Tachyzoites of the RH strain were treated for 24 h with MP-IV-1 or QQ-437 at the respective IC<sub>90</sub>. After 24 h, slides were fixed with 2% paraformaldehyde, 2.5% glutaraldehyde, 0.1 M cacodylate buffer at room temperature for 1 h. Samples were sent to be imaged in 0.1 M cacodylate buffer. They were prepared and imaged at the Albert Einstein University Analytic Imaging Facility.

**Immunofluorescence assay imaging experiments.** Wild-type RH parasites or MP-IV-1-resistant mutants were treated with MP-IV-1 for either 4 or 24 h at either the IC<sub>50</sub> or IC<sub>90</sub>. After the appropriate treatment period, slides were fixed with 3% paraformaldehyde. Slides were permeabilized with PBS–0.2% Triton X-100 at room temperature and blocked with PBS–0.2% Triton X-100–3% BSA at room temperature. For this set of experiments, dense granule antibody GRA1 (mouse) was kindly provided by Marie-France Cesbron-Delauw and Corinne Mercier (Institut Jean Roget) (4, 6), rhoptry antibody ROP13 was kindly provided by Peter Bradley (University of California Los Angeles) (46), and cathepsin antibodies (to visualize the acidocalcisome), cathepsin-like protein (CPL), and the microneme antibody M2 were kindly provided by Vern Caruthers (University of Michigan) (16), and anti-SAG1 antibody was from Invitrogen. Samples were stained with primary antibodies (GRA1, ROP13, CPL, M2, and SAG1) for 1 h and secondary antibody (mouse and rabbit) overnight.

Coverslips were mounted with Antifade (Molecular Probes, Eugene, OR), and images were analyzed by high-resolution fluorescence using deconvolution protocols. Microscopy was performed with an inverted microscope (Nikon) with a 41001 filter (excitation, 480 to 440 nm; emission, 440 nm) for fluorescein isothiocyanate (FITC), a 41035 filter (excitation, 540 to 525 nm; emission, 620 to 660 nm) for rhodamine, and a 31013v2 filter (excitation, 360 to 340 nm; emission, 460 to 450 nm) for 4',6'-diamidino-2-phenylindole (DAPI).

**ADMET.** Cytochrome P450 (CYP450) inhibition, hERGs, human liver microsomal stability, solubility, protein binding in human plasma, and permeability assays were performed as described previously (45) by Tipparaju et al. ADMET assessments for MP-IV-1 and QQ-437 were performed by Pharmaron (Louisville, KY) and Cerep (Redmond, WA), respectively.

## RESULTS

**Overview of approach and experimental design from lead identification and optimization to beginning characterization of effects of *N*-benzoyl-2-hydroxybenzamides, demonstrating how the various experiments are used in the critical path of series selection.** Herein, to identify novel leads effective against toxoplasmosis, we screened a library optimized for medicinal chemistry for compliance with Lipinski's rule of five (25). This screen of 6,811 synthetic compounds identified 28 primary "hits" with IC<sub>90</sub>s of <10  $\mu$ M. From these hits, MP-IV-1, a synthetic compound belonging to the *N*-benzoyl-2-hydroxybenzamide class, stood out as the most attractive lead for our optimization effort. MP-IV-1 was not toxic at high (10  $\mu$ M) concentrations *in vitro* and was active at low (IC<sub>90</sub> = 31 nM) concentrations *in vitro*. MP-IV-1 was effective *in vivo* in mice at reducing parasite burden. *N*-Benzoyl-2-hydroxybenzamides were synthesized by reaction of salicylamide with various acid chlorides in refluxing pyridine, purified by crystallization or preparative HPLC, and further elaborated. QQ-437 was found to be the most effective derivative of MP-IV-1. These two compounds were also tested against *Plasmodium falciparum*, a related member of the apicomplexan family and the causative agent of falciparum malaria. QQ-437 was found to be superior in efficacy to MP-IV-1, even against chloroquine-resistant parasites. We noted, however, that *N*-benzoyl-2-hydroxybenzamides may have a different target in malarial parasites, because there was a substantial dichotomy in susceptibility observed between MP-IV-1 and QQ-437 against *P. falciparum* that was not seen with *T. gondii*.

Next, an insertional mutagenesis library of *T. gondii* parasites resistant to MP-IV-1 was created (23) to begin to help us to identify the molecular target of the *N*-benzoyl-2-hydroxybenzamides in *T. gondii*. Sequencing of four clones resistant to MP-IV-1 identified an adaptin N-terminal region domain-containing protein. This suggested that the adapter protein could function in a pathway which involves the molecular target of *N*-benzoyl-2-hydroxybenzamides.

Adaptin-3 $\beta$  is part of a secretory pathway which in *T. gondii* transports critical and parasite-specific proteins through the Golgi apparatus to a series of unique organelles. These organelles include the micronemes, which secrete their contents for attachment to host cells; rhoptries, which are involved in invasion and taking over the host cell genome expression; and dense granules, which contribute their contents to the parasitophorous vacuole and also interact with host cell molecules. The mechanisms whereby proteins are directed to these organelles are only partly understood. Adaptin-1 was found to be involved in biogenesis of

rophtries (5, 34). Two other organelles, called the acidocalcisome and the plant-like vacuole (PLV), are key in calcium regulation and osmoregulation involving vacuolar ATPases, respectively, but little is known about protein trafficking to these organelles in *T. gondii*.

Adaptin-3 $\beta$  is known to target proteins to the *Arabidopsis* vacuole homologue of the *T. gondii* plant-like vacuole (1b, 2, 3, 7, 9, 11, 12, 15, 30, 39, 40, 41, 42, 43, 44). Since *T. gondii* has many plant-like features (27, 38), we explored the effects of *N*-benzoyl-2-hydroxybenzamides on the unique organelles of the *T. gondii* secretory pathway, including the PLV. The PLV can be distinguished by immunostaining with a cathepsin-like protein (35). *N*-Benzoyl-2-hydroxybenzamide-treated parasites showed disruption of repartition of micronemes, rhoptries, dense granules, and the acidocalcisome/plant-like vacuole, which is consistent with our discovery that resistant mutants had an insertion in adaptin-3 $\beta$ . The data reported here demonstrate that QQ-437 meets criteria to be a new lead compound and provide insights into a mechanism of resistance involving adaptin-3 $\beta$ , a member of the secretory pathway of *T. gondii*.

QQ-437 was found not only to be the most effective compound but also to have the best ADMET properties.

**Lead compound identification.** (i) ***N*-Benzoyl-2-hydroxybenzamides are potent compounds against *Toxoplasma* parasites.** A library of 6,811 synthetic compounds was screened against *T. gondii* tachyzoites, using a fluorescent parasite screen utilizing RH-YFP-expressing parasites (see Materials and Methods). The fluorescent parasite screen identified 28 primary hits against tachyzoites. This finding was confirmed using a [<sup>3</sup>H]uracil incorporation assay, which also serves as a measure of parasite viability as uracil becomes incorporated into nucleic acids of *T. gondii* but not its mammalian host cells. We discarded hits that displayed toxicity against host human foreskin fibroblasts (HFF). One compound stood out with robust activity and no toxicity: *N*-4-ethylbenzoyl-2-hydroxybenzamide, referred to as compound MP-IV-1 (Fig. 1A to D; Table 1), which was effective against tachyzoites *in vitro* at a concentration of 31 nM (IC<sub>90</sub>) (Fig. 1B) and showed no toxicity at the highest concentration tested (10  $\mu$ M) (Fig. 1D).

(ii) **Insertional mutagenesis provides a means to identify the molecular target pathway of MP-IV by selecting a parasite that grows slowly under compound pressure.** An insertional mutagenesis library was created to identify genes which confer resistance to MP-IV-1. This was done by transfecting the plasmid vector pLK47 (kindly provided by Laura Knoll, Madison, Wisconsin) into the *T. gondii* genome, thus disrupting the gene present at the locus where the plasmid integrated (see Fig. S1 in the supplemental material). Twenty-three mutants were cloned that were resistant to MP-IV-1 at concentrations of 10  $\mu$ M. The segment of DNA adjacent to the plasmid in the *T. gondii* genome was isolated and sequenced for four clones (see Fig. S1A).

Each of the four clones contained a disruption in the gene for an adaptin N-terminal region domain-containing protein, at bp 3170 (see Fig. S1B in the supplemental material). One of the four clones contained an additional insertion in the region of a putative dynein-1- $\alpha$  heavy-chain flagellar inner arm i1 complex. This could represent the actual target of the compound or simply mark the pathway in which the actual target resides at some point in the parasite life cycle.

The mutant parasites grew more slowly and less robustly than

the wild-type parasites (see Fig. S1C in the supplemental material).

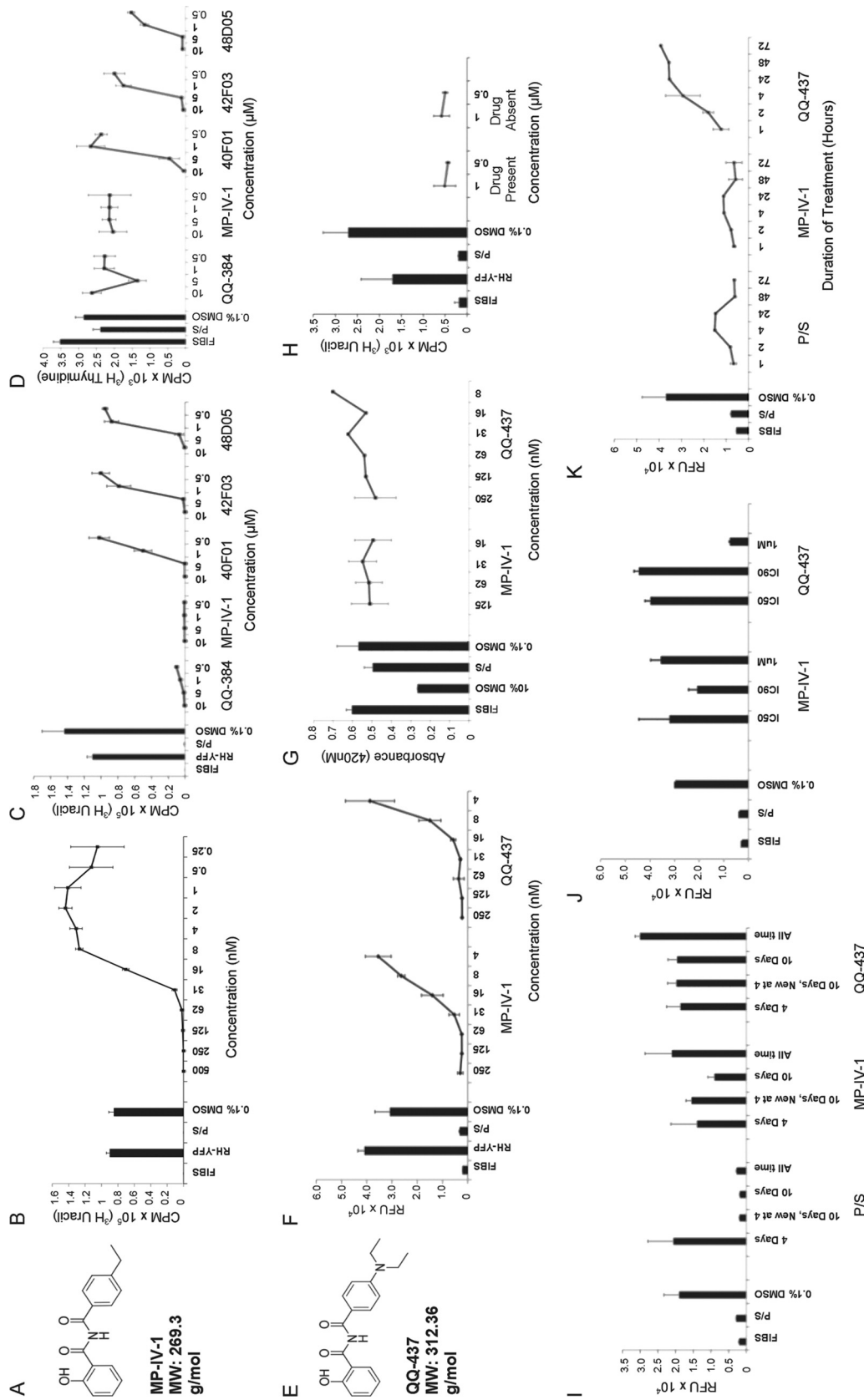
**Lead compound optimization and SAR.** Synthesis and evaluation of a wide range of MP-IV-1 derivatives yielded an optimized compound, QQ-437 (Fig. 1E and F; Table 1). The synthetic procedures, along with spectral data for this and related 2-*N*-benzoyl-2-hydroxybenzamides, are described in detail elsewhere (42a). A structure-activity relationship (SAR) study for these compounds was carried out for *T. gondii* (Table 1). Subsequent analysis of the potency of these compounds was also conducted against various strains of *P. falciparum* and pathogenic kinetoplastid parasites (Table 2) (42a). Syntheses of many of the derivative compounds and the subsequent SARs for *Leishmania*, trypanosomes, and *P. falciparum* K1 are described elsewhere (42a). Table 1 demonstrates the approach to identify an analogue with activity superior to that of QQ-437, once we determined that QQ-437 was superior to MP-IV-1. Compound QQ-437 was the most effective derivative and was more effective than MP-IV-1, demonstrating robust activity at 16 nM (IC<sub>90</sub>) and showing no toxicity at the highest concentration tested (10  $\mu$ M) (Fig. 1F and G).

Since QQ-437 is a closely related derivative of MP-IV-1, it is possible that the two compounds share a molecular target. Mutants resistant to MP-IV-1 were able to grow in the presence of QQ-437 which supports this hypothesis (data not shown). Further, since both MP-IV-1 and QQ-437 showed potent activity against tachyzoites we studied them further as representatives of the *N*-benzoyl-2-hydroxybenzamide class.

**Effects of *N*-benzoyl-2-hydroxybenzamides on *T. gondii*.** (i) **Effects on *T. gondii* *in vitro*.** To determine whether MP-IV-1 and QQ-437 inhibit intracellular parasites or invasion of host fibroblasts, parasites were allowed to infect HFF in the presence of either MP-IV-1, QQ-437, or medium. MP-IV-1 did not prevent cellular invasion but inhibited the parasite by a different mechanism (Fig. 1H), as inhibition of replication was similar with exposure to the compound before and after invasion, and inhibition was noted only after incubation of infected cells with the inhibitor.

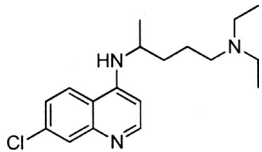
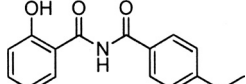
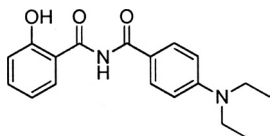
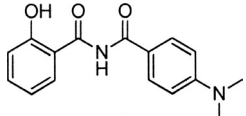
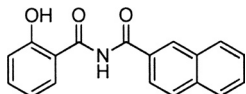
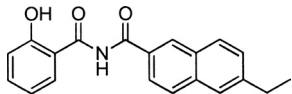
To determine whether these compounds are parasitostatic or parasitocidal, HFF infected with tachyzoites were treated with MP-IV-1 or QQ-437 or with pyrimethamine and sulfadiazine, in one of four conditions: (i) compound was present for 4 days after infection and then removed; (ii) compound was present for 4 days, replaced with fresh compound, and removed at 10 days; (iii) compound was present for 10 days and then removed; (iv) compound was present for the duration of the assay. Fluorescence measurements of the parasites were conducted daily to determine inhibition. At 14 days, levels of parasites that had been treated with MP-IV-1 or QQ-437 were similar to the levels of untreated controls, relative to the levels observed in cells treated with pyrimethamine and sulfadiazine, which remained low (Fig. 1I). Thus, MP-IV-1 and QQ-437, while inhibiting parasite proliferation, do not have a lethal effect under these conditions, as the parasite is able to grow after the compound is removed. Furthermore, the high parasite levels observed in assays where the compound was present throughout the experiment suggest that both QQ-437 and MP-IV-1 lose efficacy with time.

To confirm that observation, a standard YFP fluorescence assay was used to determine the duration of compound efficacy *in vitro*. Parasites were treated by MP-IV-1 and QQ-437 at 1  $\mu$ M and at each compound's respective IC<sub>50</sub> and IC<sub>90</sub> and imaged daily for 25 days. On day 7, all parasites treated with MP-IV-1 were at levels



**FIG 1** Imides inhibit *T. gondii* tachyzoites *in vitro*. All graphs are representative examples of replicate experiments. (A) Structure of MP-IV-1. (B) [<sup>3</sup>H]-uracil incorporation assay, with tachyzoites treated with serial dilutions of MP-IV-1 (nanomolar) to identify lowest effective concentration. CPM, counts per million scintillation. (C) Comparison of MP-IV-1 with other early hit compounds. (D) [<sup>3</sup>H]-thymidine incorporation assay to assess compound toxicity, demonstrating that the apparent inhibitory effect of some of the compounds in panel C is actually due to toxicity to host cells. (E) Structure of QQ-437. (F) Fluorescence assay to identify lowest effective concentration of QQ-437 and comparison with MP-IV-1. (G) WST-1 fluorescence assay to assess toxicity of MP-IV-1 and QQ-437 to host cells. MP-IV-1 was not tested at 250 nM in this representative graph. (H) MP-IV-1 invasion assay (via [<sup>3</sup>H]-uracil incorporation assay). (I) Fluorescence assay to determine parasitistic/parasitocidal activity of MP-IV-1 and QQ-437. In this graph, “4 Days” indicates compounds present for 4 days and then removed; “10 Days, New at 4” indicates compound removed at 10 days; “10 Days, New at 4” indicates compound removed at 10 days; and “All time” indicates compound present for duration of experiment. (J) Fluorescence assay to assess duration of compound effect. MP-IV-1 (IC<sub>50</sub>, 16 nM; IC<sub>90</sub>, 31 nM) and QQ-437 (IC<sub>50</sub>, 8 nM; IC<sub>90</sub>, 16 nM) were added once to wells infected with parasites and imaged daily. The graph is representative of day 7. (K) Fluorescence assay to assess time of effect. Parasites were treated with compound for the indicated number of hours and then the compound was removed. FIBS, uninfected fibroblasts; RH-YFP, untreated parasites; P/S, treatment with 92 μM pyrimethamine and 400 nM sulfadiazine (currently accepted medicines used to treat toxoplasmosis); 0.1% DMSO, treatment with dimethyl sulfoxide (DMSO) at the concentration used to dissolve compounds (negative control); 10% DMSO, biologically toxic concentration to assess toxicity of compounds; “Drug Present,” parasites were added to cells in the presence of MP-IV-1; and “Drug Absent,” MP-IV-1 was added after cellular invasion occurred.

TABLE 2 Effects on *Plasmodium falciparum* isolates D6 (Sierra Leone) and C235 (Thailand; chloroquine resistant)

Compound	Structure	D6			C235		
		$\mu\text{M}$	ng/ml	$r^2$	$\mu\text{M}$	ng/ml	$r^2$
Chloroquine			3.8			46.1	
MP-IV-1		2.25	604.9	0.94	>2,000		NA <sup>a</sup>
QQ-437		0.05	15.87	0.99	0.25	77.19	0.99
QQ-421		6.40	1,819	0.81	>2,000		NA
JS-2-40		1.64	476.8	0.97	4.26	1,242	0.86
JS-2-64		1.13	362.3	0.97	2.85	915.2	0.89

<sup>a</sup> NA, not available.

equivalent to those of untreated controls, as well as of parasites treated by QQ-437 at the IC<sub>50</sub> and IC<sub>90</sub>. QQ-437, however, was still effective at 1  $\mu\text{M}$  (Fig. 1J).

To determine how quickly MP-IV-1 and QQ-437 act to inhibit parasite proliferation, infected cells were treated for six different time periods before the compounds were removed and replaced with medium without compound. The compound incubation durations tested were 1, 2, 4, 24, 48, and 72 h with application of compound. After 72 h, parasite proliferation was assessed. The level of parasites in wells treated with MP-IV-1 and QQ-437 for 2 h was lower than that of untreated controls, suggesting that these two compounds act within the first 2 h to inhibit parasite proliferation (Fig. 1K).

**(ii) The *N*-benzoyl-2-hydroxybenzamides MP-IV-1 and QQ-437 are potent against *Toxoplasma* infections *in vivo*.** In order to examine the potential for using *N*-benzoyl-2-hydroxybenzamides as treatments for *T. gondii* infections, we tested the efficacy of MP-IV-1 and QQ-437 against tachyzoite infections *in vivo*. Mice were infected via intraperitoneal (IP) injection with RH strain parasites and treated daily for 6 days with IP administration of MP-IV-1 or QQ-437 at a concentration of 1, 10, or 50 mg/kg dissolved in DMSO. After 6 days, mice were euthanized, and the intraperitoneal parasite load was assessed by counting using a hemocytometer and measurements of fluorescence. Mice treated with MP-IV-1 at 50 mg/kg demonstrated significantly lower parasite counts (Fig. 2A).

The effect of MP-IV-1 on *T. gondii* tachyzoites *in vivo* was also examined using bioluminescence imaging techniques. Mice were infected intraperitoneally with 20,000 tachyzoites expressing luciferase (Fluc). These luciferase-expressing parasites provide a means to assess the parasite burden *in vivo* using a Xenogen camera, without euthanizing the mice. MP-IV-1 inhibited growth of the parasites at a concentration of 50 mg/kg, demonstrated a dose response, and was effective by day 4, with no observable signs of toxicity. The DMSO-treated control mice also were observed to have a reduction in parasite burden by day 6 due to some toxicity from DMSO needed to dissolve the compound, although less than with MP-IV-1 (Fig. 2B and C).

The effectiveness of QQ-437 against tachyzoites *in vivo* and in comparison to that of MP-IV-1 was also assessed using bioluminescence techniques. After infection with Fluc (Prugneaud type 2 stably transfected with luciferase) parasites on day one, mice were treated with QQ-437 or MP-IV-1 at a concentration of 20 mg/kg or with DMSO as an additional control. Parasite load was assessed every other day by using the Xenogen camera. Compound QQ-437 was effective in reducing parasite burden at a concentration of 20 mg/kg and was more effective than MP-IV-1 (Fig. 2D).

**(iii) *N*-Benzoyl-2-hydroxybenzamides MP-IV-1 and QQ-437 also are potent *in vitro* against *P. falciparum*, with QQ-437 having efficacy superior to that of MP-IV-1 against a chloroquine-resistant Thai parasite.** Because many compounds effective against *T. gondii* have also been found to be effective against *P.*



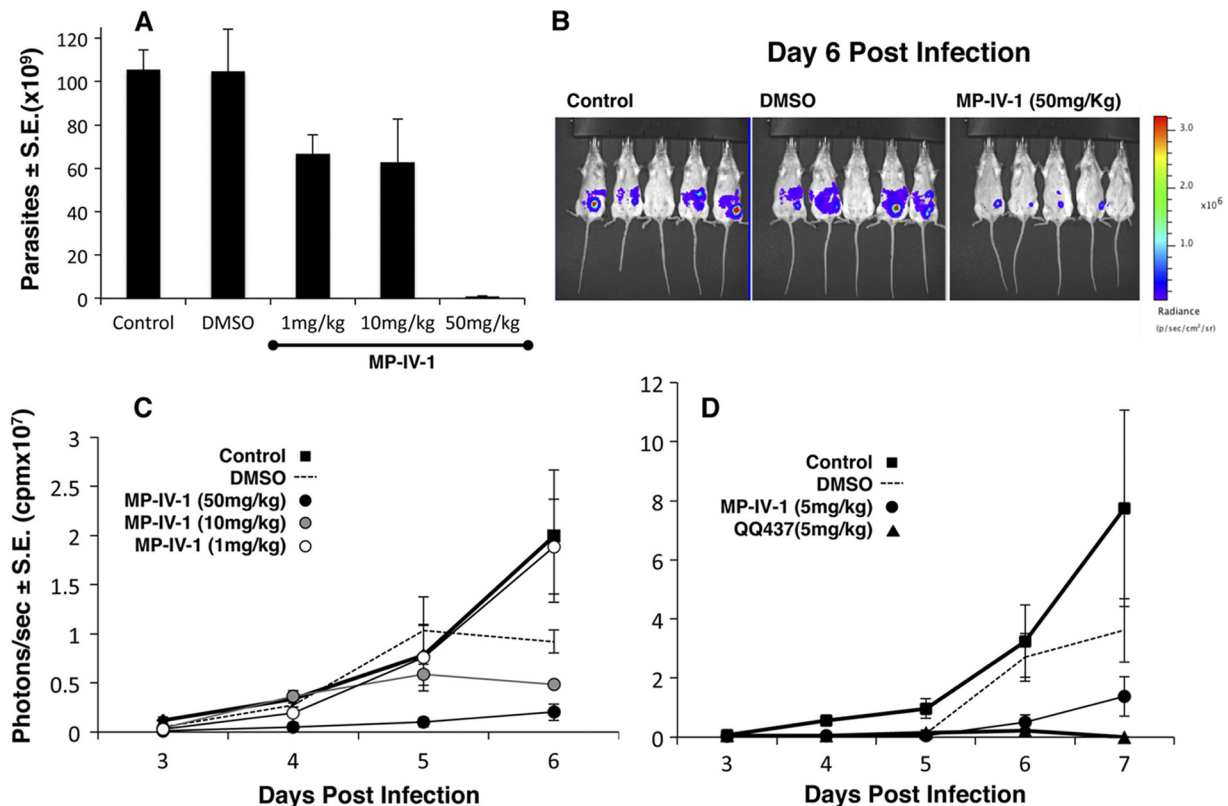


FIG 2 MP-IV-1 and QQ 437 protect mice. (A) Effect of MP-IV-1 on intraperitoneal RH tachyzoites. (B) Effect of MP-IV-1 on Fluc-expressing Prugneaud tachyzoites administered intraperitoneally, shown as Xenogen camera images. (C) Effect of MP-IV-1 over time. (D) QQ437 is more effective than MP-IV-1.

*falciparum*, we assessed the antiplasmodial effect of MP-IV-1, QQ437, and several derivatives. This was accomplished by using the malaria SYBR green I-based fluorescence assay, which is a microtiter plate drug sensitivity assay that uses the presence of malarial DNA as a measure of parasitic proliferation. The intercalation of SYBR green I dye into parasite DNA and its resulting fluorescence reflects parasite growth. Therefore, a test compound that inhibits the growth of the parasite will result in a lower fluorescence. Two strains of *P. falciparum*—D6 (CDC/Sierra Leone, chloroquine sensitive) and TM90-C235 (WRAIR, Thailand, chloroquine resistant)—were used for each compound assessment. MP-IV-1 was moderately active against D6 ( $IC_{50} = 604.9$  ng/ml) and not active against TM90-C235 ( $IC_{50} > 2000$  ng/ml). QQ-437 was active against both strains of *P. falciparum* at much lower concentrations (D6  $IC_{50} = 15.87$  ng/ml, C235  $IC_{50} = 77.19$  ng/ml). These results are summarized in Table 2. Chloroquine was used as a control for all antiplasmodial studies (Table 2).

(iv) **Electron microscopy of *N*-benzoyl-2-hydroxybenzimidate-treated *T. gondii* tachyzoites reveals disruption of dense granules, unusual lucent areas, and distortion of secretory organelles.** An electron microscopy analysis was performed to characterize the effect of MP-IV-1 and QQ-437 on the morphology of *T. gondii* parasites. Tachyzoites were treated for 24 h with either MP-IV-1 or QQ-437 at the  $IC_{90}$  and then fixed and imaged. Untreated tachyzoites cultured under the same conditions were also imaged as a basis for comparison (Fig. 3A). Both MP-IV-1 and QQ-437 appeared to affect parasite morphology in an organelle-specific manner, rather than simply causing global damage. The

nucleus, cell membrane, and rhoptries were identified in MP-IV-1- and QQ-437-treated parasites and untreated controls. However, a marked difference was seen in several organelles which receive proteins from the secretory pathway. Typical dense granules were not present in parasites treated with MP-IV-1 and QQ-437. An organelle similar in shape and size to a dense granule was visible in these samples but was much less electron dense. The acidocalcisome/PLV was missing in all MP-IV-1-treated parasites (Fig. 3B) and in many of the QQ-437 treated parasites (Fig. 3C).

(v) **Immunofluorescence assay imaging studies confirm distorted, improperly localized, and absent secretory organelles in *T. gondii* parasites treated with *N*-benzoyl-2-hydroxybenzamidates and adaptin-3 $\beta$  mutant parasites treated or not treated with *N*-benzoyl-2-hydroxybenzamidates.** Immunofluorescence staining experiments were conducted in order to confirm observations of organelle disruption seen in electron microscopy studies, as well as to investigate the differences between drug-resistant and wild-type parasites, both with and without drug pressure. Our imaging experiments were focused on several trafficking organelles implicated by association with adaptin-3 $\beta$ : micronemes, rhoptries, dense granules, and acidocalcisomes/PLVs. Wild-type RH parasites and MP-IV-1-resistant mutants were treated with MP-IV-1 for either 4 or 24 h at either the  $IC_{50}$  or  $IC_{90}$  and then incubated with antibodies to the following markers: SAG1 (surface antigen), GRA1 (dense granules), ROP13 (rhoptries), CPL (acidocalcisomes/PLVs), or M2 (micronemes). MP-IV-1 caused fragmentation and then disappearance of the acidocalcisome/PLV and also resulted in marked distortion of immunostaining of

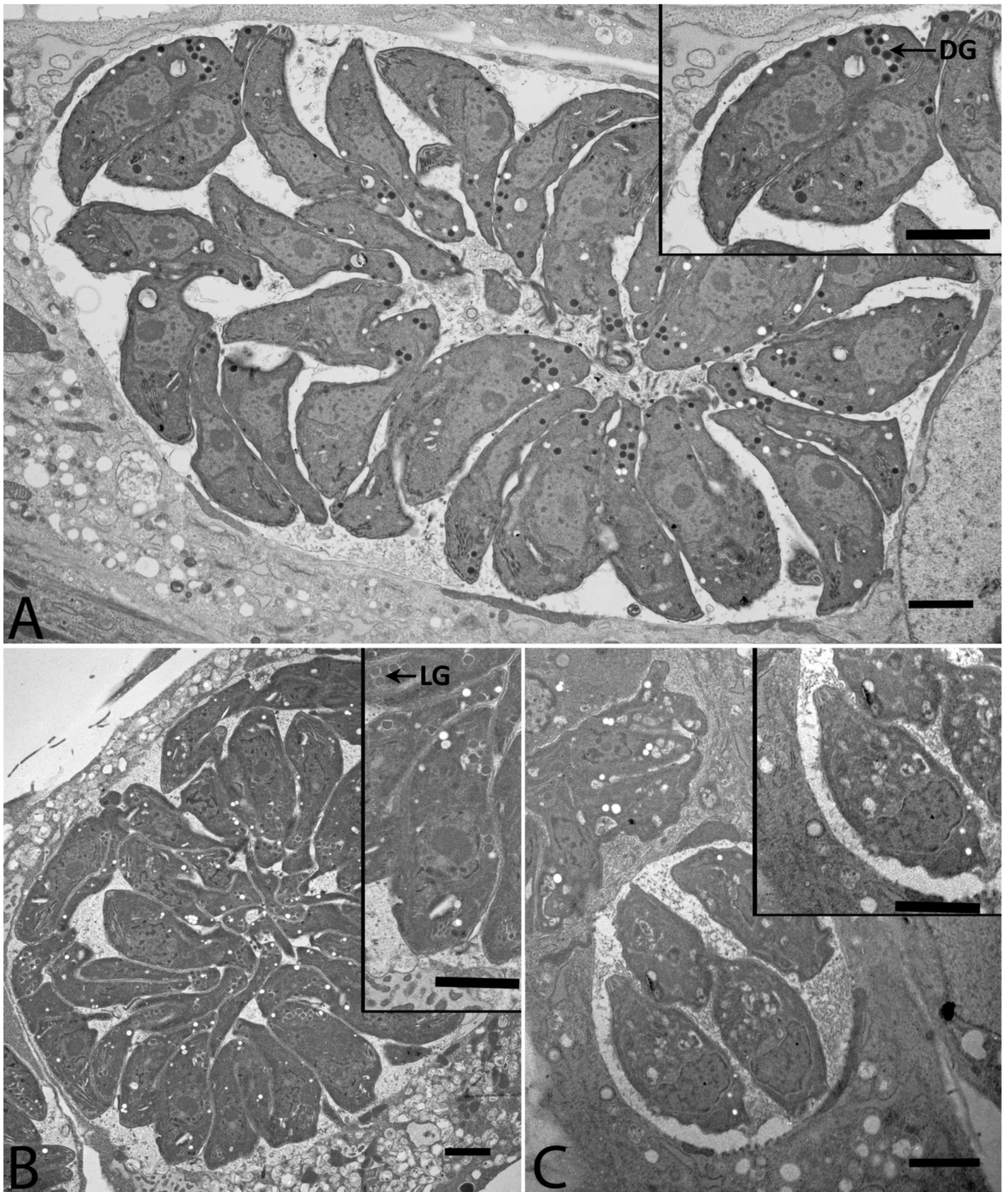


**FIG 3** Electron microscopy images showing loss of dense granule content and acidocalcisomes after treatment with imides. (A) Wild-type, untreated RH tachyzoite parasites. (Inset) Enlargement. Note normal ultrastructure. DG, dense granules. (B) Tachyzoites treated with MP-IV-1. (C) Tachyzoites treated with QQ-437. Note the absence of dense granules with normal ultrastructure and density in *N*-benzoyl-2-hydroxybenzamide-treated parasites. LG, light granules.

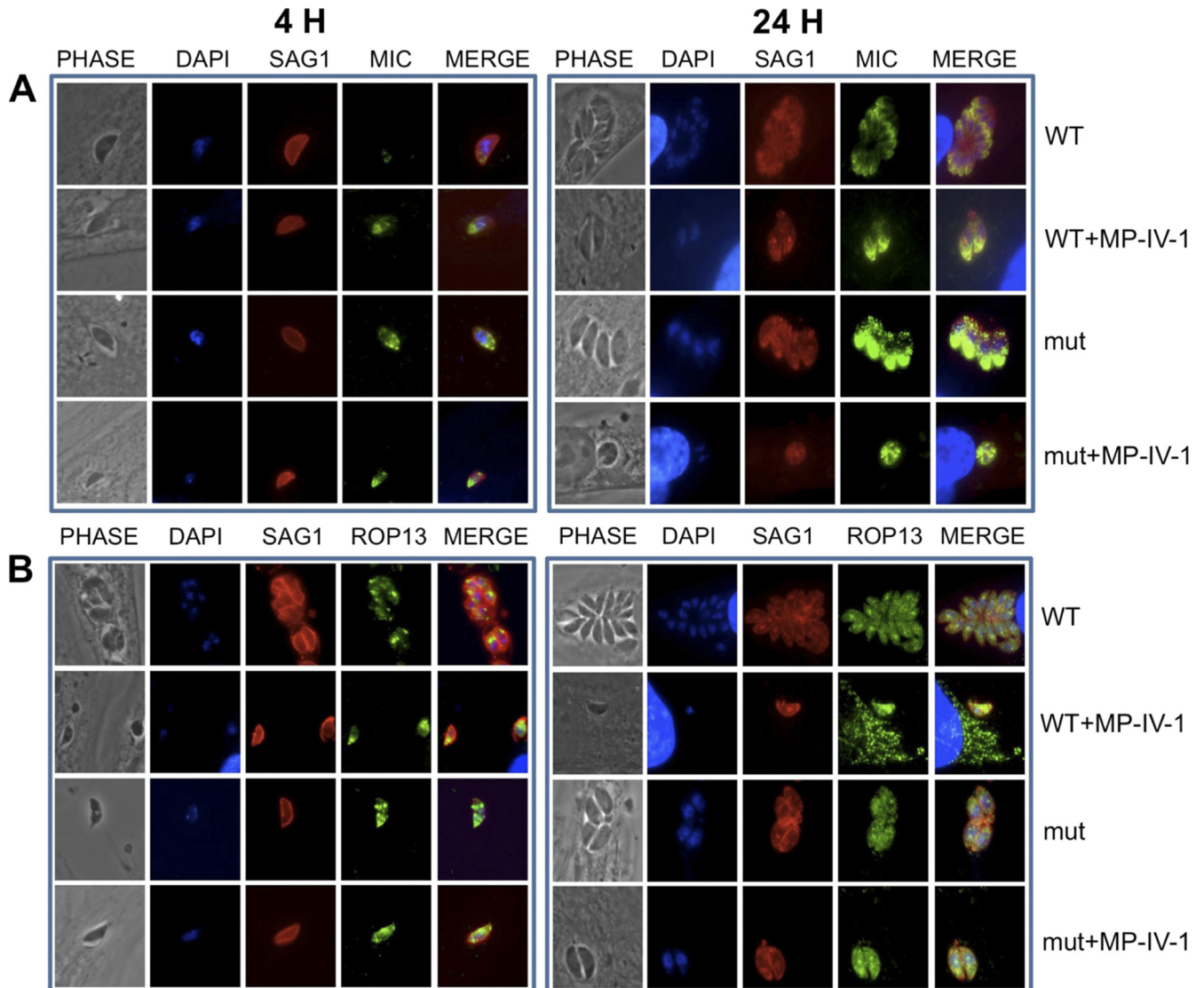


**FIG 4** Immunofluorescence staining experiments confirm observations of organelle disruption seen in electron microscopy studies, demonstrating differences between *N*-benzoyl-2-hydroxybenzamide-resistant and wild-type parasites, both with and without *N*-benzoyl-2-hydroxybenzamide pressure. The images show that the imides target the secretory pathway and that the acidocalcisome/plant-like vacuole is lost with this treatment and other secretory organelles develop unusual morphology and function. Organelles whose contents are secreted and thereby implicated in association with adaptin-3 $\beta$  include rhoptries, acidocalcisomes/plant-like vacuoles, micronemes, and dense granules. There is marked distortion of secretory organelles, including micronemes (A), rhoptries (B), functional dense granules (C), and fragmentation and then disappearance of the acidocalcisome/plant-like vacuole (D). These abnormalities were present at 4 h and more pronounced at 24 h. Mutant parasites exhibited a similar phenotype, with more pronounced abnormalities being seen in MP-IV-1-treated mutants, with the exception of dense granule proteins reaching the parasitophorous vacuole in the mutants. These results demonstrate an effect of MP-IV-1 on organelles that receive proteins via the secretory pathway, with the most profound effect being on the acidocalcisome/plant-like vacuole. Abbreviations for antibody labeling of parasite surface or organelle: SAG1, surface antigen; GRA1, dense granules; ROP13, rhoptries; CPL, acidocalcisome/plant-like vacuole; and M2, micronemes. (E) Immunostaining for enoyl reductase, which demonstrates that the plastid may be modestly elongated in the MP-IV-1-treated parasites, especially at 24 h. Since targeting to the plastid differs from targeting to secretory organelles, this may be a secondary effect. This finding is subtle and not marked as for the micronemes, rhoptries, dense granules, and acidocalcisome/plant-like vacuole. (F) Higher magnification of merged images of acidocalcisomes/PLVs (immunostained with antibody to CPL), rhoptries (immunostained with antibody to ROP13), and micronemes (immunostained with antibody to MIC2) in wild-type (WT), *N*-hydroxy-2-benzamide-treated wild-type parasites (WT+MP-IV-1), insertional mutants (mut), and mutant parasites treated with *N*-hydroxy-2-benzamide (mut+MP-IV-1).

other secretory organelles, including micronemes, rhoptries, and functional dense granules. These abnormalities were present at 4 h and were more pronounced at 24 h (Fig. 4A to F). The mutant parasites exhibited a similar phenotype, with more pronounced abnormalities being seen in the MP-IV-1-treated mutants. One exception was that dense granule proteins may have reached the

parasitophorous vacuole of the mutant parasites (Fig. 4). These results demonstrate the effect of MP-IV-1 on organelles that receive proteins via the secretory pathway, with the most profound effect being on the acidocalcisome/PLV. An antibody to enoyl reductase appeared to demonstrate a subtle increase in size for the plastid, especially at 24 h (Fig. 4E).

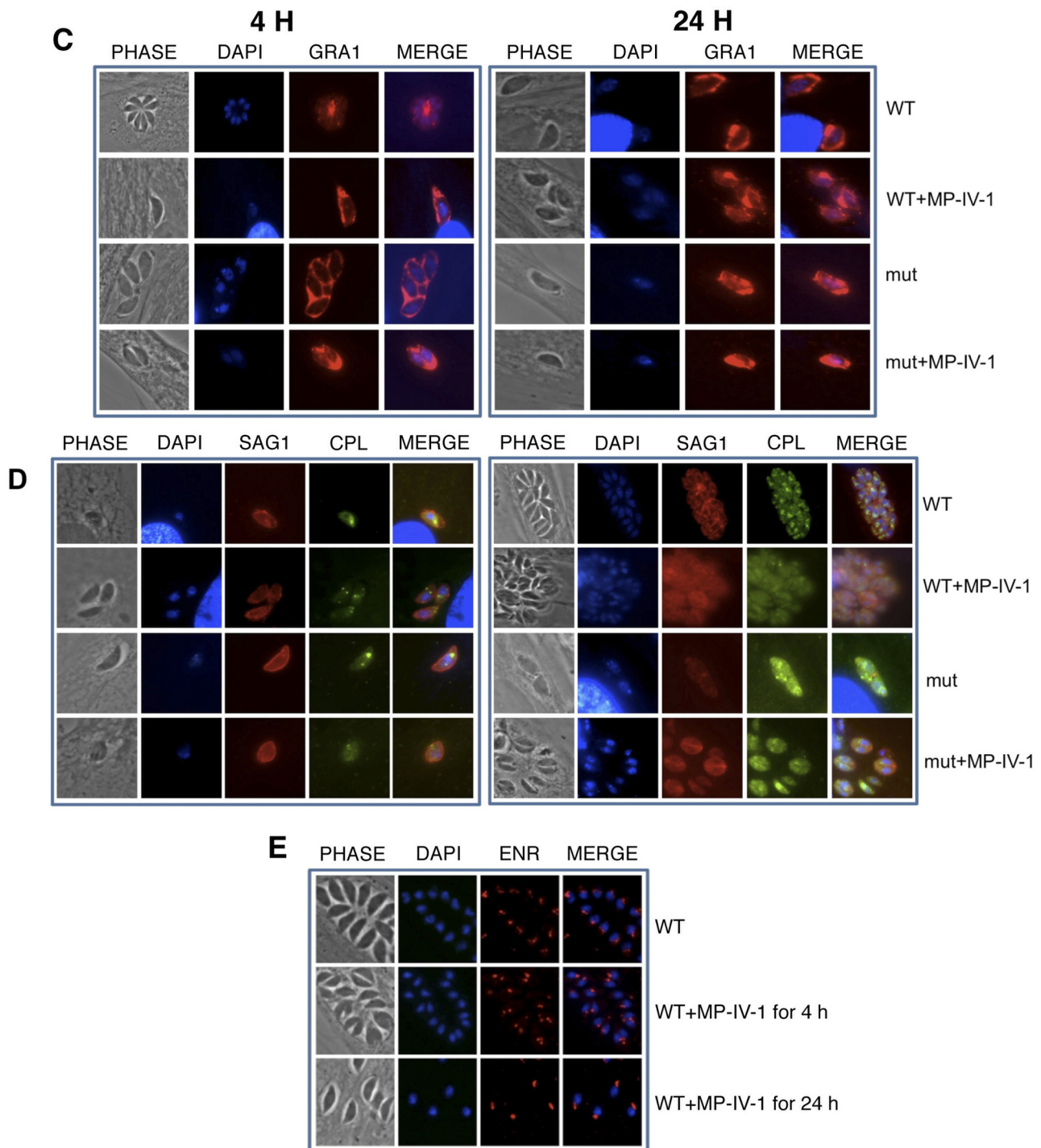


FIG 4 Continued

**Sequence alignment of *T. gondii* adaptin-3 $\beta$  with *Arabidopsis* and other protozoan and human adaptin-3 $\beta$ s.** Multi-sequence alignments that relate *T. gondii* adaptin-3 $\beta$  to those of other species are shown in Fig. S1 and S2 in the supplemental material. The *T. gondii* and *Neospora caninum* adaptin-3 $\beta$ s are almost identical. The *Arabidopsis* adaptin-3 $\beta$  has a number of similarities (see Fig. S2), some not present in human adaptin-

3 $\beta$ , particularly at *T. gondii* amino acid numbers 17 to 21, 210 to 221, 427 and 428, 446 to 450, 591 to 600, 670 to 674, and 1182 to 1188 (see Fig. S2). There are some areas in the parasite adaptin-3 $\beta$ s that are relatively conserved compared with the human adaptin-3 $\beta$ , including those at *T. gondii* amino acids 321 to 332 and 689 to 691 (see Fig. S2). Overall analysis of the sequence alignment for a number of different AP-3 $\beta$  sequences shows a low degree of

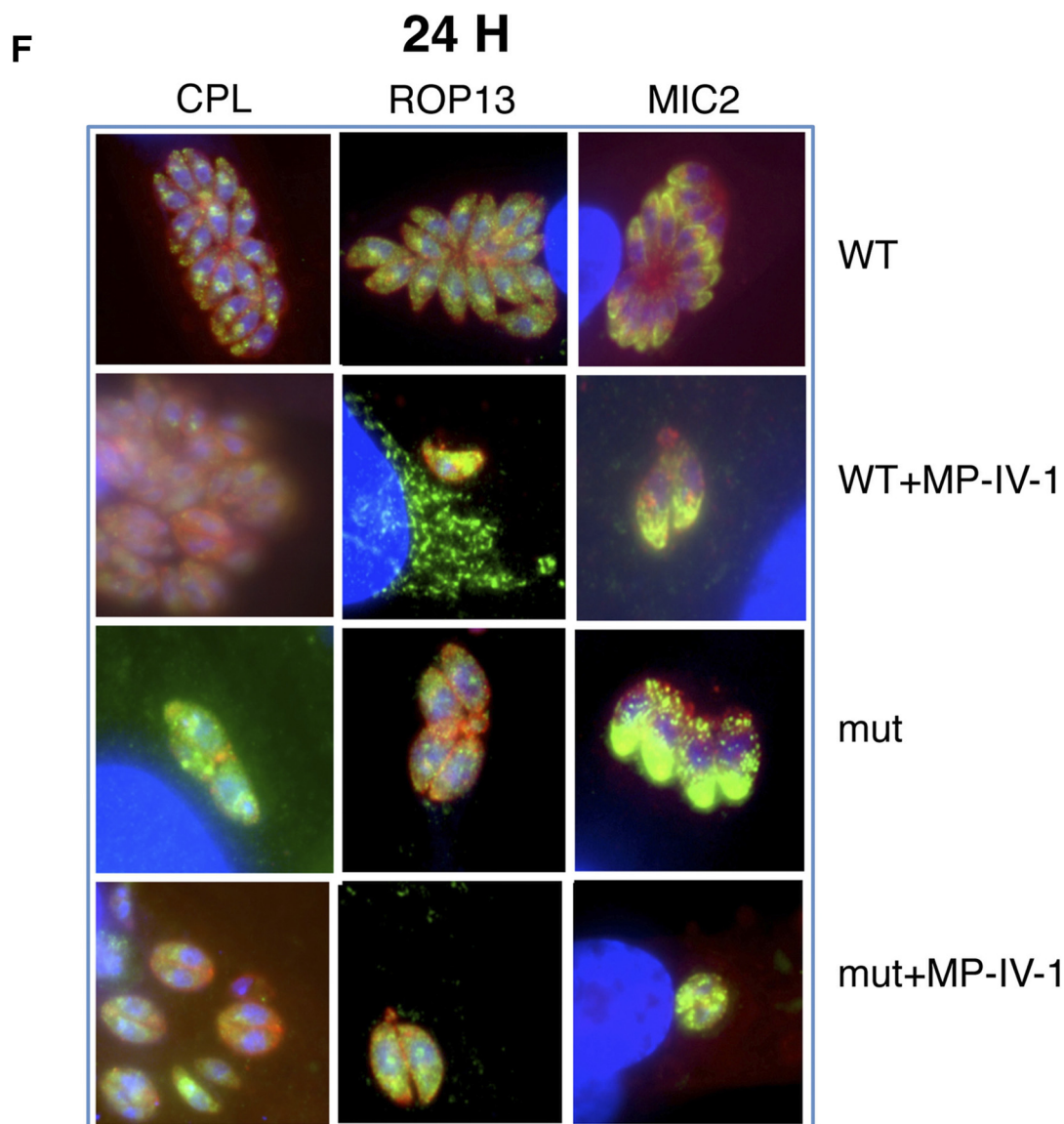


FIG 4 Continued

sequence identity across the family, particularly at the C-terminal region.

**Comparison of ADMET properties of MP-IV-1 and QQ-437.** These promising biological data led to our next experiments determining the ADMET and pharmacokinetics properties of MP-IV-1 (Table 3). MP-IV-1 showed acceptable aqueous solubility but also showed high plasma protein binding (99.86%) with poor permeability, as determined by lipid parallel artificial membrane permeability assay (PAMPA) ( $103.77\% \pm 1.78\%$  recovery), and with an apparent log  $P$  value of  $-4.64$ . MP-IV-1 also showed inhibition of CYP2C9 (71.32% at  $10 \mu\text{M}$ ) but not CYP2D6 and CYP3A4. No hERG inhibition was observed. Although chemical stability was acceptable, the metabolic stability of this compound was poor. MP-IV-1 was metabolized quickly in liver microsomes with a half-life less than 10 min. Only 1.58% remained after 30 min incubation with microsomes. MP-IV-1 was also degraded in human liver microsomes without NADPH, which suggests that

MP-IV-1 may be metabolized not only by CYP450- and FMO-mediated biotransformation but also by other enzymes such as hydrolases, including amidases. An *in vivo* pharmacokinetics (PK) study was conducted, and similar problems with metabolic stability were observed. In mice, less than 1% of the parent compound remained in the plasma after intravenous injection of 5 mg/kg. The metabolic stability problems associated with MP-IV-1 are most likely caused by an unstable imide linker in the compound.

Further ADMET assessments were conducted on our most potent compound, QQ-437, using metabolic stability assays and P-cytochrome inhibition assays. We hypothesized that the imide linker in QQ-437 would be more stable than that of MP-IV-1 due to the electron-donating effect of the diethylamine substituent in ring B, which should contribute to the stabilization of the imide linker. QQ-437 was much more stable than MP-IV-1 in a human liver microsome assay with a half-life of approximately 33 min with moderate metabolism in human hepatocytes. QQ-437 did not show

TABLE 3 ADMET-PK assays

Assay	Unit(s)	Value for:	
		MP-IV-1	QQ-437
Aqueous solubility (pH 7.4)	$\mu\text{M}$	50.82	ND <sup>a</sup>
Plasma protein binding by ultrafiltration	Mean % bound measured	99.86	ND
Lipid-PAMPA	–Log P app <sup>b</sup>	4.64 $\pm$ 0.06 <sup>c</sup>	ND
	% recovery	103.77 $\pm$ 1.78 <sup>c</sup>	ND
CYP2C9 inhibition	% inhibition at 10 $\mu\text{M}$	71.32	22
CYP2D6 inhibition	% inhibition at 10 $\mu\text{M}$	15.50	–3
CYP3A4 inhibition	% inhibition at 10 $\mu\text{M}$	–7.69	–1
Cell-based hERG screening	IC <sub>50</sub> ( $\mu\text{M}$ )	>300	ND
Chemical stability	% remaining after 60 min	100	ND
Human liver microsome stability	% remaining after 30 min	1.58	53.6
	Half-life (min)	<10	33
Human liver microsome stability (without NADPH)	% remaining after 30 min	88.2	ND
Human hepatocyte stability	% remaining after 60 min	ND	23
Mouse intravenous plasma concn (at 5 mg/kg)	ng/ml after 0.083 h	2,343	ND
	ng/ml after 0.25 h	335	ND
	ng/ml after 0.5 h	108	ND
	ng/ml after 1 h	28.4	ND

<sup>a</sup> ND, not done.

<sup>b</sup> –Log P app, where P app is the apparent permeability, in cm/s.

<sup>c</sup> Values are means  $\pm$  standard deviations.

significant inhibition of any of the three P cytochromes tested (CYP2C9, CYP2D6, and CYP3A4), which is an important quality of a lead medicine candidate. Compared with MP-IV-1, QQ-437 is a superior, more potent inhibitor with a better ADMET profile.

## DISCUSSION

These studies define the *N*-benzoyl-2-hydroxybenzamides as a class of compounds that are effective at a low nanomolar range against *T. gondii* tachyzoites by interacting with a novel secretory pathway to the acidocalcisome/plant-like vacuole and dense granules. Our screen of a library of 6,811 compounds against *T. gondii* tachyzoite replication identified *N*-4-ethylbenzoyl-2-hydroxybenzamide (MP-IV-1) as an inhibitor of *T. gondii* tachyzoites, effective at 31 nM (IC<sub>90</sub>) *in vitro* with no toxicity to host fibroblasts at the highest concentration tested (10  $\mu\text{M}$ ) and effective *in vivo* against *T. gondii* in mice at 50 mg/kg.

Derivatives of MP-IV-1 were created and tested *in vitro*, and compound QQ-437 was found to be more effective than any of them, being active at 16 nM (IC<sub>90</sub>) *in vitro*, with no signs of toxicity at 10  $\mu\text{M}$ . *In vivo* experiments in mice demonstrated that QQ-437 is effective against tachyzoites at 20 mg/kg. Although the structure of MP-IV-1 displayed similarities to that of the important enoyl reductase inhibitor triclosan, enzymatic assays demonstrated that this compound did not inhibit enoyl reductase (data not shown).

After performing our medium throughput screen, which identified our lead compound without prior assumptions, we found that a similar *N*-benzoyl-2-hydroxybenzamide had been reported in a patent (36a) as a less-than-optimal inhibitor of *P. falciparum*. Coincidentally, earlier we had found that salicylhydroxamic acid (SHAM), a related compound which is partly contained in the *N*-benzoyl-2-hydroxybenzamides, was noted to inhibit *T. gondii*, *P. falciparum*, and *C. parvum* (37a). Nonetheless, *N*-benzoyl-2-hydroxybenzamide QQ437 is a novel compound. We synthesized QQ437 in our SAR and discovered in the experiments described herein that this is the best of the compounds to inhibit *T. gondii* as well as *P. falciparum* Thailand and Sierra Leone strains. The SAR

that led to our discovery and the development of the compounds in this family is also novel and has not been described previously.

Our genome-wide investigations revealed a specific mechanism of resistance mediated by the adaptin-3 $\beta$  protein. Adaptin proteins, specifically AP-3 $\beta$ , are found in the trans-Golgi network and endosomal membranes and have been implicated in the transportation of proteins between the two compartments (1b, 2, 3, 7, 9, 11, 12, 15, 30, 40, 41, 42, 43, 45). The role of AP3 $\beta$  as a cargo protein prompted an investigation of the effect of MP-IV-1 on parasite morphology, in particular the trafficking to secretory pathway organelles. It is not clear at this time what the role of this protein is in the components of the endomembrane trafficking machinery and pathogenesis. Recent work with *Arabidopsis* has provided insight into the interaction of AP-3 $\beta$  with other components of the secretory pathway (summarized in reference 15).

To provide further data on the effects of *N*-benzoyl-2-hydroxybenzamides on *T. gondii*, electron microscopy studies were performed which demonstrated that treatment with MP-IV-1 and QQ-437 had a profound effect on dense granules and acidocalcisomes/plant-like vacuoles. The effects of these compounds were localized and organelle specific, as the nucleus, rhoptries, and membranes remained distinguishable.

Immunofluorescence assays also demonstrated that these compounds interfere with formation of the acidocalcisome/plant-like vacuole and interfere with proper targeting to secretory organelles, including rhoptries, micronemes, and dense granules. This demonstrates the targeting of this secretory pathway by these novel imides. It will be of interest to further characterize, with electron micrographs, the ultrastructure of the mutant parasites along with conditional mutants (20a) of adaptin-3 $\beta$  and other possible molecular targets. Another molecular target might be identified by click chemistry and pull-down studies. These data will add to our immunofluorescent-antibody study of the subcellular organelles in the mutant and compound-treated parasites.

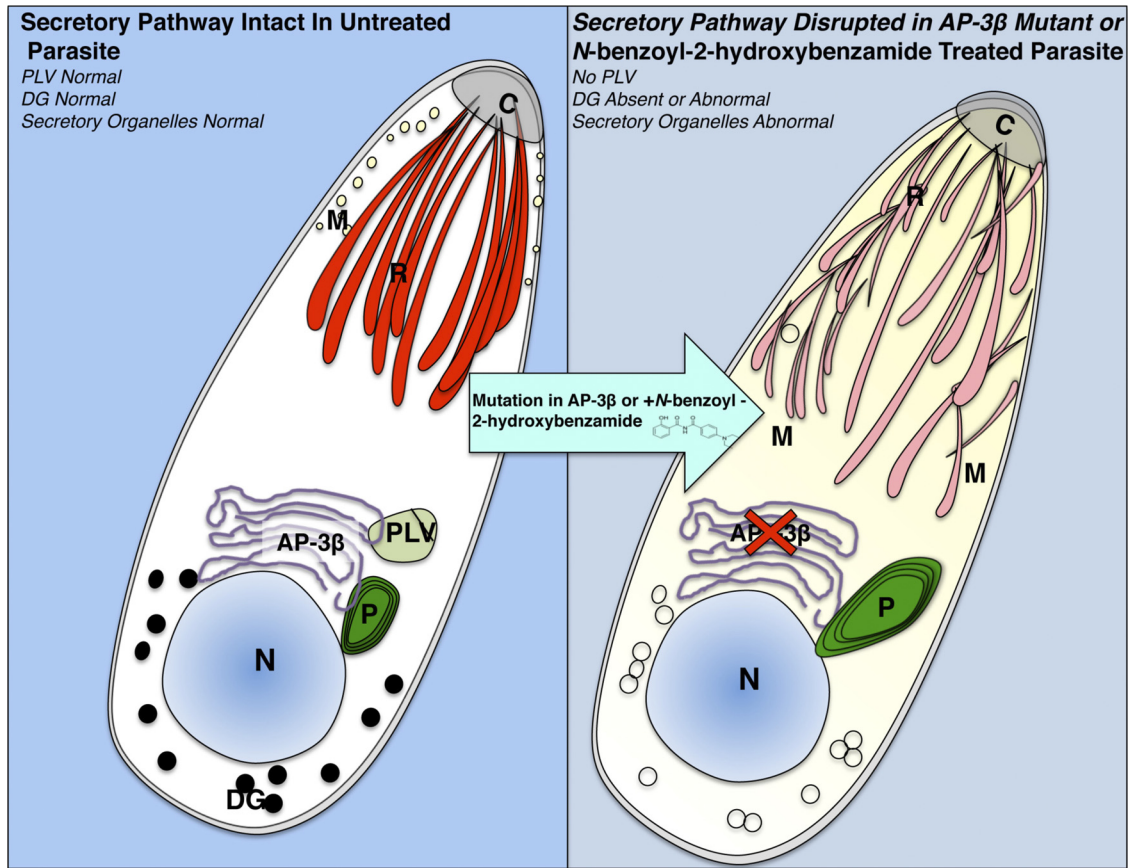


**FIG 5** Schematic diagram of the unique adaptin-3 $\beta$  secretory pathway that traffics proteins to the plant-like vacuole (PLV) and dense granules identified through the discovery that novel *N*-benzoyl-2-hydroxybenzamides can treat *T. gondii* infections. (Left) *Toxoplasma* proteins have normal trafficking through the secretory pathway via adaptin-3 $\beta$  to PLV and other organelles that receive proteins from the secretory pathway (R, rhoptries; M, micronemes; DG, dense granules; PLV, acidocalcisome/plant-like vacuole). This trafficking takes place through the Golgi apparatus (G). N, nucleus; C, conoid; P, plastid. The arrow shows the addition of *N*-benzoyl-2-hydroxybenzamide or an insertional mutation in adaptin-3 $\beta$  that causes the same phenotype. (Right) Secretory pathway. Adaptin-3 $\beta$  has an insertional mutation, or the secretory pathway is interacting with *N*-benzoyl-2-hydroxybenzamides. QQ-437, the most active of the *N*-benzoyl-2-hydroxybenzamides, interacts with and inhibits a protein in the secretory pathway, perhaps adaptin-3 $\beta$  or another protein, causing a phenotype similar to that caused by the mutation in adaptin-3 $\beta$ . These compounds or an insertional mutation interferes with sorting in the late endosomal compartment. Disappearance of the PLV and dense granule contents and mistargeting to other secretory organelles occurs. The secretory pathway is disrupted. The red X over adaptin-3 $\beta$  shows the effect of the mutation or interaction of the secretory pathway with *N*-benzoyl-2-hydroxybenzamide.

Adaptin-3 $\beta$  is a 3.6-kbp protein encoded on chromosome 11. In other organisms, adaptins are involved in membrane trafficking, selecting cargo for incorporation into trafficking vesicles, in the form of four distinct adaptin complexes. Adaptin-3 proteins are involved in other organisms in transport between the trans-Golgi network and the endosomes. Adaptin-1 is the only *T. gondii* adaptin characterized to date and has been found to be important in *T. gondii* rhoptry biogenesis (34). Adaptin-3 $\beta$  has been found to be present in *Leishmania* (10). The adaptin proteins play a critical role in the Apicomplexa for the underlying cell biology of invasion via biogenesis of the rhoptries (i.e., adaptin-1 [34]) and potentially other aspects involved with membrane trafficking (19). In elegant studies with *Trypanosoma brucei*, adaptin-3 $\beta$  was recently reported to be critical for biogenesis of this kinetoplastid's acidocalcisome (20), which is consistent with the findings herein for *T. gondii*. The multisequence alignments in Fig. S1 and S2 in the supplemental material show differences and similarities of adaptin-3 $\beta$ s in different species. *Neospora caninum* has the most similar adaptin-3 $\beta$  to that of *T. gondii*. Our studies indicate that a mutation in adaptin-3 $\beta$  causes the parasite to replicate more

slowly than wild-type parasites, and this parasite can survive treatment with the *N*-benzoyl-2-hydroxybenzamides. This does not, however, indicate that adaptin-3 $\beta$  is the molecular target of *N*-benzoyl-2-hydroxybenzamides. It is also possible that the insertional mutant and the inhibition studies simply reveal the phenotype of a common pathway in which the target molecule functions. For example, a microneme or other protein traversing the secretory pathway might interact with *N*-benzoyl-2-hydroxybenzamides. The complex could then obstruct the secretory pathway or other molecules interacting with adaptin-3 $\beta$ . Potentially, phosphorylation and ubiquitination may play a role in adaptin-3 $\beta$  interactions with the secretory pathway as binding sites, as both are present in other adaptins (17, 18, 26, 37).

Experiments testing *N*-benzoyl-2-hydroxybenzamides against two strains of *P. falciparum* showed that QQ-437, while not as effective as the established medicine chloroquine, was able to inhibit the parasite at low concentrations. MP-IV-1 was less effective, but it did show modest activity against the D6 Sierra Leone chloroquine-sensitive strain but not the TM90-C235 Thailand chloroquine-resistant strain. This indicates that these inhibitory

compounds may have potential targets in other apicomplexan parasites as well. It does not imply, however, that the molecular target is the same. In fact MP-IV-1, has been reported to inhibit *P. falciparum* by targeting heme detoxification protein synthesis (21). *P. falciparum* has been described to lack adaptin-3 $\beta$  and to have a secretory pathway that diverges from that of other apicomplexan parasites (8, 33). The effect of QQ-437 as an antiplasmodial compound has been confirmed in the studies with *P. falciparum* strain K1, which is also a chloroquine-resistant parasite (42a). In this study, with these compounds, *Leishmania*, which does have an adaptin-3 $\beta$ , was susceptible to another imide (42a). *Neospora* and *Eimeria* also appear to have adaptin-3 $\beta$ s, and there is homology to the *T. gondii* and *Arabidopsis thaliana* adaptin-3 $\beta$ s, another plant-like feature of this apicomplexan parasite.

It will be of interest to determine whether QQ-437 has any effect against bradyzoites. Currently we are developing model systems to test effects of compounds on bradyzoite molecular targets. We are using the following methods for these assays: conditional tetracycline repressor modulation and other means to knock out bradyzoite and tachyzoite targets (20a) *in vitro* and *in vivo*, treatment of parasites in tissue culture that are in the encysted bradyzoite stage, and treatment of parasites in the bradyzoite stage *in vivo*. If the mechanism of action of the *N*-hydroxyl-2-hydroxybenzamides is the inhibition of the secretory pathway to the plant-like vacuole, which appears to be essential for withstanding stress by the parasite, as well as other secretory organelles, it is possible that the compounds might inhibit bradyzoites better than tachyzoites. Alternatively, if these compounds only slow replication and create a stress response by interfering with the secretory pathway without killing the parasite, it is possible that they would eliminate only tachyzoites in the presence of a competent immune response. We demonstrated this type of effect when we eliminated ribosomal protein S13 (RPS13), leading to G<sub>0</sub> arrest and exit from the cell cycle. In tissue culture, conditional knockdown of RPS13 was not lethal. It resulted in dormant parasites which could persist for many months *in vitro* (20a). However, in mice, knockdown of *T. gondii* RPS13 created a remarkably effective vaccine (20a). There was no persistence of the vaccine or challenge organism, presumably because the immune system eliminated the vaccine parasites that were arrested in G<sub>0</sub> and thereby elicited a robust immune response sufficient to clear the homologous parent strain challenge. If the latter was the case for our compounds, they might be useful only for causing replication arrest in tachyzoites. If this proved to be the case in future studies *in vivo*, then perhaps the compound could be accompanied by a compound that inhibits a stress-related kinase, such as EIF kinase (43a) or bradyzoite Apetela 2 or other essential bradyzoite transcription factors (1, 1a, 20a). Inhibitors of egress, cell cycle, or stress responses described previously (23a, 32a, 32b, 34a, 43a, 47) might be compounds that could work together with this class of compounds. This would allow elimination and treatment of both tachyzoites and dormant organisms. We also are studying whether a delivery mechanism such as the transductive peptides we described earlier (40a) could facilitate access to the bradyzoites within cysts for additional small molecules besides triclosan or antisense compounds which could eliminate or interfere with all molecular targets.

Identifying vulnerable molecular targets in *T. gondii* and developing effective medicines against them can ultimately help the development of medicines against other apicomplexan parasites which may share similar molecular targets and pathways. *N*-Ben-

zoyl-2-hydroxybenzamide and its novel derivative QQ-437 represent a family of compounds that affect *T. gondii*. Resistance to *N*-benzoyl-2-hydroxybenzamides occurs when a trafficking protein, adaptin-3 $\beta$  is interrupted. This suggests that the molecular target utilizes or is part of this secretory pathway. Definitive target identification will require additional work. The optimization and derivatization of these compounds, as well as further exploration of their molecular target, holds the promise of a new family of medicines which might be further improved or lead to discoveries of other novel compounds to treat the devastating diseases toxoplasmosis as well as to impact diseases caused by other protozoan parasites. In our discovery of the molecular target pathway effected by this new class of compounds, we also identified the endocytic/exocytic hub where sorting of proteins targeted to various organelles occurs. In their earlier work, Rohloff et al., Docampo et al., and others (13, 14, 20, 24, 31, 39) discovered and characterized an important protozoan compartment with these putative or proven functions. Our work herein indicates that adaptin-3 $\beta$  appears to act in the sorting to this compartment that regulates ions and/or as a post-Golgi sorting compartment for secretory proteins destined for the dense granules, micronemes, rhoptries, and acidocalcisomes/plant-like vacuoles in *T. gondii*.

#### ACKNOWLEDGMENTS

This work was supported by NIAID NIH DMID U01 AI082180, the Institute for Genomics, Genetics, and Systems Biology, University of Chicago, and by gifts from the Mann and Cornwell, Taub, Rooney-Alden, Engel, Pritzker, Harris, Zucker, and Mussilami families. S.P.M. is supported by an MRC Career Development fellowship.

We thank Marie-France Cesbron-Delauw and Corrine Mercier for providing  $\alpha$ GRA1, Vern Carruthers for providing  $\alpha$ CPL and  $\alpha$ MIC, Peter Bradley for providing  $\alpha$ ROP13, Laura Knoll for providing the PLK insertional mutagenesis construct, The Albert Einstein Electron Microscopy Core Facility for preparation of electron micrographs, and Matthias Dean Carpentier and Daniel Lee for assistance with preparation of figures. We also very much appreciate the suggestions and advice of NIH Program Officer John Rogers and SAB members David Jacobus, Clark Eid, John McCall, and Marie-France Cesbron-Delauw throughout the syntheses, work, and analyses in these studies.

There are no conflicts of interest.

The opinions of researchers at Walter Reed Army Institute of Research are their own and do not reflect the views of the U.S. Army or the Department of Defense.

#### REFERENCES

- Behnke MS, et al. 2010. Coordinated progression through two subtranscriptomes underlies the tachyzoite cycle of *Toxoplasma gondii*. *PLoS One*. 25:e12354.
- Behnke MS, et al. 2008. The transcription of bradyzoite genes in *Toxoplasma gondii* is controlled by autonomous promoter elements. *Mol. Microbiol.* 68:1502–1518.
- Benková E, et al. 2003. Local, efflux-dependent auxin gradients as a common module for plant organ formation. *Cell* 115:591–602.
- Blilou I, et al. 2005. The PIN auxin efflux facilitator network controls growth and patterning in *Arabidopsis* roots. *Nature* 433:39–44.
- Boehm M, Bonifacino JS. 2002. Genetic analyses of adaptin function from yeast to mammals. *Gene* 286:175–186.
- Braun L, et al. 2008. Purification of *Toxoplasma* dense granule proteins reveals that they are in complexes throughout the secretory pathway. *Mol. Biochem. Parasitol.* 157:13–21.
- Breinich MS, et al. 2009. A dynamin is required for the biogenesis of secretory organelles in *Toxoplasma gondii*. *Curr. Biol.* 19:277–286.
- Cesbron-Delauw MF, et al. 1989. Molecular characterization of a 23-kilodalton major antigen secreted by *Toxoplasma gondii*. *Proc. Natl. Acad. Sci. U. S. A.* 86:7537–7541.



7. Cowles CR, Odorizzi G, Payne GS, Emr SD. 1997. The AP-3 adaptor complex is essential for cargo-selective transport to the yeast vacuole. *Cell* 91:109–118.
8. Dacks JB, Poon PP, Field MC. 2008. Phylogeny of endocytic components yields insight into the process of nonendosymbiotic organelle evolution. *Proc. Natl. Acad. Sci. U. S. A.* 105:588–593.
9. Dell'Angelica EC, Shotelersuk V, Aquilar RC, Gahl WA, Bonifacino JS. 1999. Altered trafficking of lysosomal proteins in Hermansky-Pudlak Syndrome due to mutations in the  $\beta$ 3A subunit of the AP-3 adaptor. *Mol. Cell* 3:11–21.
10. Denny PW, Morgan GW, Field MC, Smith DF. 2005. *Leishmania* major: clathrin and adaptin complexes of an intra-cellular parasite. *Exp. Parasitol.* 109:33–37.
11. Dettmer J, Hong-Hermesdorf A, Stierhof YD, Schumacher K. 2006. Vacuolar H<sup>+</sup>-ATPase activity is required for endocytic and secretory trafficking in *Arabidopsis*. *Plant Cell* 18:715–730.
12. Dhonukshe P, et al. 2008. Generation of cell polarity in plants links endocytosis, auxin distribution and cell fate decisions. *Nature* 456:962–966.
13. Docampo R, Jimenez V, King-Keller S, Li ZH, Moreno SN. 2011. The role of acidocalcisomes in the stress response of *Trypanosoma cruzi*. *Adv. Parasitol.* 75:307–324.
14. Docampo R, Moreno SN. 2011. Acidocalcisomes. *Cell Calcium* 50:113–119.
15. Feraru E, et al. 2010. The AP-3  $\beta$  adaptin mediates the biogenesis and function of lytic vacuoles in *Arabidopsis*. *Plant Cell* 22:2812–2824.
16. Gaji RY, Flammer HP, Carruthers VB. 2011. Forward targeting of *Toxoplasma gondii* propeptides to the micronemes involves conserved aliphatic amino acids. *Traffic* 12:840–853.
17. Geyer M, Fackler OT, Peterlin BM. 2002. Subunit H of the V-ATPase involved in endocytosis shows homology to  $\beta$ -adaptins. *Mol. Biol. Cell* 13:2045–2056.
18. Happel N, et al. 2004. *Arabidopsis* mu A-adaptin interacts with the tyrosine motif of the vacuolar sorting receptor VSR-PS1. *Plant J.* 37:678–693.
19. Hoppe HC, Ngô HM, Yang M, Joiner KA. 2000. Targeting to rhoptry organelles of *Toxoplasma gondii* involves evolutionarily conserved mechanisms. *Nat. Cell Biol.* 2:449–456.
20. Huang G, et al. 2011. Adaptor protein-3 (AP-3) complex mediates the biogenesis of acidocalcisomes and is essential for growth and virulence of *Trypanosoma brucei*. *J. Biol. Chem.* 286:36619–36630.
- 20a. Hutson SL, et al. 2010. T. gondii RP promoters and knockdown reveal molecular pathways associated with proliferation and cell-cycle arrest. *PLoS One* 5:e14057.
21. Jani D, et al. 2008. HDP—a novel heme detoxification protein from the malaria parasite. *PLoS Pathog.* 4:1–15.
22. Johnson JD, et al. 2007. Assessment and continued validation of the malaria SYBR green I-based fluorescence assay for use in malaria drug screening. *Antimicrob. Agents Chemother.* 51:1926–1933.
23. Knoll LJ, Furie GL, Boothroyd JC. 2001. Adaptation of signature-tagged mutagenesis for *Toxoplasma gondii*: a negative screening strategy to isolate genes that are essential in restrictive growth conditions. *Mol. Biochem. Parasitol.* 116:11–16.
- 23a. Larson ET, et al. 2009. *Toxoplasma gondii* cathepsin L is the primary target of the invasion-inhibitory compound morpholinurea-leucyl-homophenyl-vinyl sulfone phenyl. *J Biol Chem.* 284:26839–26850.
24. Li ZH, et al. 2011. Hyperosmotic stress induces aquaporin-dependent cell shrinkage, polyphosphate synthesis, amino acid accumulation and global gene expression changes in *Trypanosoma cruzi*. *J. Biol. Chem.* 286:43959–43971.
25. Lipinski CA, Lombardo F, Dominy BW, Feeney PJ. 2001. Experimental and computational approaches to estimate solubility and permeability in drug discovery and development settings. *Adv. Drug Deliv. Rev.* 46:3–26.
26. Mattera R, Tsai YC, Weissman AM, Bonifacino JS. 2006. The Rab5 guanine nucleotide exchange factor Rabex-5 binds ubiquitin (Ub) and functions as a Ub ligase through an atypical Ub-interacting motif and a zinc finger domain. *J. Biol. Chem.* 281:6874–6883.
27. McLeod R, et al. 2001. Triclosan inhibits the growth of *Plasmodium falciparum* and *Toxoplasma gondii* by inhibition of apicomplexan Fab I. *Int. J. Parasitol.* 31:109–113.
28. McLeod R, et al. 2006. Outcome of treatment for congenital toxoplasmosis, 1981–2004: the National Collaborative Chicago-Based, Congenital Toxoplasmosis Study. *Clin. Infect. Dis.* 42:1383–1394.
29. McLeod R, et al. 2006. Severe sulfadiazine hypersensitivity in a child with reactivated congenital toxoplasmic chorioretinitis. *Pediatr. Infect. Dis. J.* 25:270–272.
30. Meyer DM, et al. 2005. Oligomerization and dissociation of AP-1 adaptors are regulated by cargo signals and by ArfGAP1-induced GTP hydrolysis. *Mol. Biol. Cell* 16:4745–4754.
31. Miranda K, et al. 2010. Characterization of a novel organelle in *Toxoplasma gondii* with similar composition and function to the plant vacuole. *Mol. Microbiol.* 76:1358–1375.
32. Mui EJ, et al. 2008. Novel triazine JPC-2067-B inhibits *Toxoplasma gondii* in vitro and in vivo. *PLoS Negl Trop. Dis.* 2:e190.
- 32a. Nagamune K, Xiong L, Chini E, Sibley LD. 2008. Plants, endosymbionts and parasites: abscisic acid and calcium signaling. *Commun. Integr. Biol.* 1:62–65.
- 32b. Nagamune K, et al. 2008. Abscisic acid controls calcium-dependent egress and development in *Toxoplasma gondii*. *Nature* 456:207–210.
33. Nevin WD, Dacks JB. 2009. Repeated secondary loss of adaptin complex genes in the Apicomplexa. *Parasitology* 139:86–94.
34. Ngô HM, et al. 2003. AP-1 in *Toxoplasma gondii* mediates biogenesis of the rhoptry secretory organelle from a post-Golgi compartment. *J. Biol. Chem.* 278:5343–5352.
- 34a. Ojo KK, et al. 2010. *Toxoplasma gondii* calcium-dependent protein kinase 1 is a target for selective kinase inhibitors. *Nat. Struct. Mol. Biol.* 5:602–607.
35. Parrusini F, Coppens I, Shah PP, Diamond SL, Carruthers VB. 2010. Cathepsin L occupies a vacuolar compartment and is a protein maturase within the endo/exocytic system of *Toxoplasma gondii*. *Mol. Microbiol.* 76:1340–1357.
36. Plouffe D, et al. 2008. *In silico* activity profiling reveals the mechanism of action of antimalarials discovered in a high-throughput screen. *Proc. Natl. Acad. Sci. U. S. A.* 105:9059–9064.
- 36a. Rathore D, Jani D, Nagarkatti R. June 2007. Novel therapeutic target for protozoal diseases. US patent 20070148185(A1).
37. Ricotta D, Hansen J, Preiss C, Teichert D, Höning S. 2008. Characterization of a protein phosphatase 2A holoenzyme that dephosphorylates the clathrin adaptors AP-1 and AP-2. *J. Biol. Chem.* 283:5510–5517.
- 37a. Roberts CW, et al. 2004. Evidence for mitochondrial-derived alternative oxidase in the apicomplexan parasite *Cryptosporidium parvum*: a potential anti-microbial agent target. *Int. J. Parasitol.* 34:297–308.
38. Roberts F, et al. 1998. Evidence for the shikimate pathway in apicomplexan parasites. *Nature* 393:801–805.
39. Rohloff P, et al. 2011. Calcium uptake and proton transport by acidocalcisomes of *Toxoplasma gondii*. *PLoS One* 6:e18390.
40. Rojo E, Gillmor CS, Kovaleva V, Somerville CR, Raikhel NV. 2001. Vacuoleless1 is an essential gene required for vacuole formation and morphogenesis in *Arabidopsis*. *Dev. Cell* 1:303–310.
- 40a. Samuel BU, et al. 2003. Delivery of antimicrobials into parasites. *Proc. Natl. Acad. Sci. U. S. A.* 100:14281–14286.
41. Sanmartín M, et al. 2007. Divergent functions of VTI12 and VTI11 in trafficking to storage and lytic vacuoles in *Arabidopsis*. *Proc. Natl. Acad. Sci. U. S. A.* 104:3645–3650.
42. Somerville CR, et al. 2008. The secretory system of *Arabidopsis*. In Somerville CR, Meyerowitz EM (ed), *The Arabidopsis book*. American Society of Plant Biologists, Rockville, MD.
- 42a. Stec J, et al. 21 February 2012, posting date. Synthesis, biological evaluation and structure-activity relationships of N-benzoyl-2-hydroxybenzamides as agents active against *P. falciparum* (K1 strain), trypanosomes, and *Leishmania*. *J. Med. Chem.* doi:10.1021/jm2015183.
43. Stepp JD, Huang K, Lemmon SK. 1997. The yeast adaptor protein complex, AP-3, is essential for the efficient delivery of alkaline phosphatase by the alternate pathway to the vacuole. *J. Cell Biol.* 139:1761–1774.
- 43a. Sullivan WJ, Jr, Narasimhan J, Bhatti MM, Wek RC. 2004. Parasite-specific eIF2 (eukaryotic initiation factor-2) kinase required for stress-induced translation control. *Biochem J.* 380:523–531.
44. Surpin M, et al. 2003. The VTI family of SNARE proteins is necessary for plant viability and mediates different protein transport pathways. *Plant Cell* 15:2885–2899.
45. Tipparaju SK, et al. 2010. Identification and development of novel inhibitors of *Toxoplasma gondii* enoyl reductase. *J. Med. Chem.* 53:6287–6300.
46. Turetzky JM, Chu DK, Hajagos BE, Bradley PJ. 2010. Processing and secretion of ROP13: a unique *Toxoplasma* effector protein. *Int. J. Parasitol.* 40:1037–1044.
47. Vonlaufen N, Naguleswaran A, Coppens I, Sullivan WJ, Jr. 2010. MYST family lysine acetyltransferase facilitates ataxia telangiectasia mutated (ATM) kinase-mediated DNA damage response in *Toxoplasma gondii*. *J. Biol. Chem.* 285:11154–11161.